(12) INTERNATIONAL APPLICATION PUBLISHED UNDER THE PATENT COOPERATION TREATY (PCT)

(19) World Intellectual Property Organization
International Bureau

(43) International Publication Date
22 September 2016 (22.09.2016)

WIPO | PCT

(10) International Publication Number
WO 2016/145539 A1

(51) International Patent Classification:
G01N 27/30 (2006.01) *G01N 27/36* (2006.01)
G01N 21/66 (2006.01) *G01N 27/403* (2006.01)
G01N 21/76 (2006.01)

(21) International Application Number:
PCT/CA2016/050314

(22) International Filing Date:
18 March 2016 (18.03.2016)

(25) Filing Language: English

(26) Publication Language: English

(30) Priority Data:
62/134,809 18 March 2015 (18.03.2015) US
62/200,156 3 August 2015 (03.08.2015) US

(71) Applicant: **THE ROYAL INSTITUTION FOR THE ADVANCEMENT OF LEARNING/MCGILL UNIVERSITY** [CA/CA]; 845 Sherbrooke Street West, Montréal, Québec H3A 0G4 (CA).

(72) Inventors: **MAUZEROLL, Janine**; 1009 Hôtel de Ville, Montréal, Québec H2X 3A4 (CA). **DANIS, Laurence**; 3410 rue Rushbrooke, Montréal, Québec H4G 1S7 (CA). **NOYHOUZER, Tomer Aharon**; 5337 Rue Chambord, Montréal, Québec H2J 3N4 (CA). **SNOWDEN, Michael Edward**; 3495 rue Dezery (Apt 8), Montréal, Québec H1W 2S8 (CA). **TEFASHE, Ushula Mengesha**; 5510-106 avenue Robinson, Côte Saint-Luc, Québec H4V 2P5 (CA).

(74) Agent: **NORTON ROSE FULBRIGHT CANADA LLP/S.E.N.C.R.L., S.R.L.**; 1, Place Ville Marie, bureau 2500, Montréal, Québec H3B 1R1 (CA).

(81) Designated States *(unless otherwise indicated, for every kind of national protection available)*: AE, AG, AL, AM, AO, AT, AU, AZ, BA, BB, BG, BH, BN, BR, BW, BY, BZ, CA, CH, CL, CN, CO, CR, CU, CZ, DE, DK, DM, DO, DZ, EC, EE, EG, ES, FI, GB, GD, GE, GH, GM, GT, HN, HR, HU, ID, IL, IN, IR, IS, JP, KE, KG, KN, KP, KR, KZ, LA, LC, LK, LR, LS, LU, LY, MA, MD, ME, MG, MK, MN, MW, MX, MY, MZ, NA, NG, NI, NO, NZ, OM, PA, PE, PG, PH, PL, PT, QA, RO, RS, RU, RW, SA, SC, SD, SE, SG, SK, SL, SM, ST, SV, SY, TH, TJ, TM, TN, TR, TT, TZ, UA, UG, US, UZ, VC, VN, ZA, ZM, ZW.

(84) Designated States *(unless otherwise indicated, for every kind of regional protection available)*: ARIPO (BW, GH, GM, KE, LR, LS, MW, MZ, NA, RW, SD, SL, ST, SZ, TZ, UG, ZM, ZW), Eurasian (AM, AZ, BY, KG, KZ, RU, TJ, TM), European (AL, AT, BE, BG, CH, CY, CZ, DE, DK, EE, ES, FI, FR, GB, GR, HR, HU, IE, IS, IT, LT, LU, LV, MC, MK, MT, NL, NO, PL, PT, RO, RS, SE, SI, SK, SM, TR), OAPI (BF, BJ, CF, CG, CI, CM, GA, GN, GQ, GW, KM, ML, MR, NE, SN, TD, TG).

Published:

— *with international search report (Art. 21(3))*

(54) **Title**: ELECTROCHEMICAL FLOW CELL AND ULTRAMICROELECTRODE

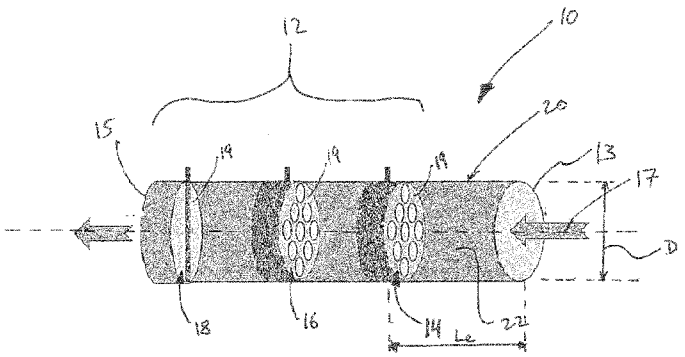

Figure 1

(57) **Abstract**: An electrochemical flow cell is described which includes a flow passage extending between the inlet and outlet to define a flow path for fluid to flow through the cell body as fully developed laminar flow. A number of flow-through electrodes are disposed within the flow passage. The flow-through electrodes are arranged in serial flow succession within the flow passage and have a plurality of apertures therein through which the fluid passes. The working electrode is positioned within the flow passage at a predetermined distance downstream of the inlet of the cell body which corresponds to a streamwise location at which substantially fully developed laminar flow occurs. At least the working electrode of the flow cell may comprise an ultramicroelectrode that is manufactured as described herein. However, this ultramicroelectrode, whether single or multicore, may also be used for applications other than the described flow cell.

WO 2016/145539 A1

ELECTROCHEMICAL FLOW CELL AND ULTRAMICROELECTRODE

TECHNICAL FIELD

[001] The present disclosure relates generally to systems for electroanalysis, and more particularly to electrochemical flow cells, ultramicroelectrodes, and methods for manufacturing each.

BACKGROUND

[002] Very generally speaking, an electrochemical flow cell comprises several electrodes, such as a working electrode, and auxiliary electrode and a reference electrode, which work together with an electrochemical detector to apply a controlled electrical potential for a sample fluid to flow across.

[003] Flow systems which employ electrochemical flow cells are well known and may offer a number of advantages in comparison to static liquid processes, such as the automation of continual and batch measurements, and permit stages of liquid replacements and automated mixing. The use of such electrochemical flow cells may thus permit the precision and accuracy of the measurements in electroanalysis to be improved, as better control and optimization of the process is possible.

[004] Electrochemical flow systems also permit the control of mass transport for analytical studies and a number of other applications. For example, a high rate of mass transport can be used to study reaction kinetics for homogeneous and heterogeneous reactions. The majority of commercially available electrochemical flow systems rely on flow injection analysis (FIA) combined with either "jet-flow" (sometimes called "wall-jet") or "flow-by" methodologies in the electrochemical flow cells. Improved electrochemical flow cells are therefore sought.

[005] These electrochemical flow cells include a number of electrodes. For certain applications of such electrochemical flow cells wherein the flow cells are microscopic in size, correspondingly micro-scale electrodes, or ultramicroelectrodes (UMEs) may

therefore be employed. Improved UMEs may also be sought, whether to be used in electrochemical flow cells or in other electrochemical applications.

[006] UMEs are defined as electrodes with at least one dimension smaller than $25\mu m$. Apart from their small dimensions they may offer several advantages including, for example, high sensitivity, fast steady state response, low double-layer charging currents, high scan rates and small ohmic losses. Furthermore, their small current requirements enable electrochemical measurements in low conductive media, e.g. organic solvents, where the voltage drop associated with high solution resistance makes these experiments difficult for convention electrodes.

[007] Common geometries of such UMEs include disk, hemispherical, inlaid ring, ring-disk, and finite conical. The most frequently used geometry for UMEs is disk, whereby an electroactive material is embedded within an outer insulating layer. UMEs have been used in a variety of applications including biological systems, charge transport at liquid/liquid interfaces, and corrosion studies.

[008] However, the fabrication of high quality UMEs with a controlled geometry is a difficult and time-consuming process, which requires experimental skill and patience. A critical geometric parameter affecting the overall quality of the UME is the RG, which is defined as the ratio between the radius of the insulating sheath (r_T) and the radius of electroactive surface (a).

[009] UMEs with small RG are essential in scanning electrochemical microscopy (SECM) in order to reduce tip-to-substrate distance (d), allowing for a higher sensitivity. The RG also has a significant effect on the current recorded during SECM approach curve measurements. A smaller RG will result in a larger current at short tip-to-substrate distances (<5) because of enhanced contributions from back diffusion of the mediator. They also decrease the probability of contact between the insulating sheath of the UME and the sample, which experimentally occurs upon axial misalignment of the UME.

[0010] The fabrication of known disk UMEs has focused on gold or platinum disk UMEs, which required labour intensive processes and limited ability to batch process and/or automate their manufacture.

[0011] Accordingly, it would be beneficial to provide a fabrication methodology for UMEs that reduces the fabrication time, provides highly reproducible UME geometries, and allows for a wide range of electroactive materials including platinum and gold but also silver, mercury, and carbon fiber. It would be further beneficial for the UME manufacturing methodology to be applicable to microreference electrodes, such as but not limited to, $Ag/AgCl$ microreference electrodes, and to electrodes which may be used in electrochemical flow cells.

SUMMARY OF THE INVENTION

[0012] There is therefore provided an electrochemical flow cell comprising: a cell body having an inlet, an outlet, and a flow passage extending between the inlet and outlet to define a flow path for fluid flowing through the cell body; a number of flow-through electrodes disposed within the cell body and in said flow passage, the flow path extending through said flow-through electrodes, which each have an electrode surface disposed transverse to a flow direction along the flow path through the flow passage, said flow-through electrodes arranged in serial flow succession within the flow passage and including at least an upstream working electrode, a downstream reference electrode, and a counter electrode disposed between the working electrode and the reference electrode, the flow-through electrodes having a plurality of apertures therein through which the fluid passes; and wherein the working electrode is positioned within the flow passage at a predetermined distance downstream of the inlet of the cell body, said predetermined distance corresponding to a streamwise location at which substantially fully developed laminar flow of the fluid flowing along the flow path through the cell body.

[0013] The electrochemical flow cell as defined above may have a flow passage that is free of flow disturbances to generate substantially fully developed laminar flow

throughout the flow passage of the flow cell, from at least the upstream working electrode and the outlet of the flow passage.

[0014] The flow passage of the electrochemical flow cell as defined above may be substantially circular in cross-sectional shape and defines a diameter.

[0015] The predetermined distance of the electrochemical flow cell as defined above may have an entrance length (Le) of the flow passage, wherein the entrance length (Le) is determined as: Le= 0.06 * Re * D, where Re is the Reynolds Number and D is the diameter of the circular flow passage.

[0016] The flow-through electrodes of the electrochemical flow cell as defined above may have flow-facing electrode surfaces that are symmetrical about two perpendicular planes of symmetry.

[0017] At least the working electrode and the counter electrode may have honeycomb configurations, and may be honeycomb screen-printed electrodes.

[0018] These honeycomb configurations of the working electrode and the counter electrode may define a plurality of individual passages that extend in a direction of the flow path between the flow-facing electrode surfaces on an upstream side and a downstream surface on an opposite side of the flow-through electrodes, the individual passages providing substantially uninterrupted fluid flow therethrough.

[0019] The electrode surfaces of said electrodes in the electrochemical flow cell as defined above may be disposed perpendicularly to the flow direction through the flow passage.

[0020] The electrochemical flow cell may be modular, permitting a number of said electrochemical flow cells to be interconnected with each other.

[0021] The electrochemical flow cell may be operable to simultaneously acquire absorbance and electrochemiluminescence (ECL) measurements.

[0022] A hydrodynamic electrochemiluminescence (ECL) device comprising the electrochemical flow cell as defined above may also be provided, wherein the electrochemical flow cell generates an electrochemiluminescence (ECL) signal.

[0023] A method of obtaining at least one of electrochemical and spectroscopic measurements from respective sensor may also be provided, which includes connecting the electrochemical flow cell as defined above to the respective sensor in electrical flow communication and generating a fluid flow through the electrochemical flow cell.

[0024] A flow system in connection with the electrochemical flow cell as defined above may further comprise a spectroscopic sensing module having a spectroscopic detector in communication with at least the working electrode.

[0025] A flow system in connection with the electrochemical flow cell as defined above may further comprise an electrochemical sensing module in communication with at least the working electrode, the electrochemical sensing module being configured to perform at least one of potentiometric, galvanostatic, and impedance based electrochemical measurements.

[0026] In accordance with another aspect, there is also provided a method of manufacturing an ultramicroelectrode, comprising: pulling a capillary according to a predetermined pulling profile, the predetermined pulling profile applying substantially equal tensile forces to each of the opposed ends of the capillary in opposite directions to form a narrowed neck in the capillary, the narrowed neck defining a capillary wall that is symmetrical relative to a longitudinal axis extending centrally through the capillary at the narrowed neck thereof; severing the narrowed neck of the capillary to form two separate micropipette tips, each having an opening symmetrically defined within the capillary walls; inserting an electroactive wire into the opening defined within the capillary wall of at least one of the tip ends formed from the pulled capillary; and sealing the tip end having the electroactive wire inserted therein by applying heat to fuse the electroactive wire within the surrounding capillary walls.

[0027] In the method as defined above, the step of severing the narrowed neck of the capillary may include at least one of applying the tensile forces until the capillary breaks at the narrowed neck and breaking the narrowed neck of the pulled capillary at predetermined position.

[0028] In the method as defined above, breaking the narrowed neck may further comprise applying local heat to the predetermined position heat using a laser.

[0029] The method as defined above may further comprise forming the ultramicroelectrode to have a ratio of a radius of the capillary wall to a radius of the electroactive wire at the tip end of less than 10. This ratio may more particularly be from 2.5 to 3.6, and more particularly still may be about 3.

[0030] In the method as defined above, the step of sealing may include using a fusion process wherein a temperature based fusion of the capillary to the electroactive wire occurs.

[0031] The method as defined above may further comprise selecting the electroactive wire to be one of a metal wire or a fiber wire.

[0032] The method as defined above may further comprise severing the narrowed neck of the capillary at a substantial midpoint thereof.

[0033] A method of forming a multicore ultramicroelectrode using the method of as defined above is also provided, wherein the capillary is a soft glass capillary, and the method further comprises inserting multiple electroactive wires into the soft glass capillary after the steps of pulling and severing.

[0034] The method as defined above may further comprise using electrodeposition on an exposed surface of the electroactive wire to form a hemispherical tip of the ultramicroelectrode.

[0035] The method as defined above may further comprise providing the capillary with a plurality of bores extending therethrough.

[0036] In accordance with another aspect of the present disclosure there is also provided a method of manufacturing a multicore ultramicroelectrode comprising: pulling a double-barrel soft glass capillary of predetermined inner and outer diameters according to a predetermined pulling profile; pulling until the capillary breaks at the reduced neck producing two pulled pipette with a sealed extremity with two separate compartment; at least one of pulling until the capillary breaks at the reduced neck producing two pulled pipettes and breaking the pulled capillary at the reduced neck at predetermined position; inserting a predetermined length of wire or fiber into one of the two compartment of the reduced neck of the pulled capillary and a predetermined length of a silver wire in the second one; sealing the pulled capillary to the wire or the fiber and the silver wire via a predetermined fusion process; exposing the electroactive surface of the UME; and depositing silver chloride on the exposed silver disk

[0037] In accordance with a further alternate aspect of the present disclosure, there is provided a method of manufacturing a multicore ultramicroelectrode comprising: at least one of pulling and molding a glass preform having a predetermined outer geometry and a plurality of bores of predetermined inner diameters according to either a predetermined profile or a predetermined event occurs; inserting a predetermined length of at least one of the wire and the fiber into at least one reduced bore of the plurality of bores; and sealing the at least one reduced bore to the at least one of the wire and the fiber via a predetermined fusion process.

[0038] In accordance with a further alternate aspect of the present disclosure, there is provided a modular device for controlling fluid flow to electrochemical and spectroscopic sensors may also be provided which comprises: an inlet system, where laminar pipe flow is established; and a flow through electrochemical sensing module with well-defined hydrodynamics; and a spectroscopic sensing module for measuring at the electrode surface; and an outlet system for the removal of solution.

[0039] The device as defined above may further incorporate an electrode assembly within the electrochemical sensing module, which may be configured to perform potentiometric, galvanostatic, and/or impedance based electrochemical measurements.

[0040] Multiple electrochemical sensors can be also be combined to create sensor arrays or generator-collector electrode assemblies.

[0041] The electrochemical module within the flow cell can be used with different electrochemical flow techniques, e.g. continual flow, fluid injection, stop-flow.

[0042] The device may also provide a modular component which houses a spectroscopic detector, focused upon the electrode.

[0043] Different types of spectroscopic measurements may thus be supported.

[0044] There is also provided an electrochemical device that can perform both electrochemical and spectroscopic measurements. The measurements can be performed simultaneously or individually.

[0045] The outlet module of the device described above may help remove waste fluid and does not allow the egress of measured sample back to the areas of detection.

[0046] The device as described above may be suitable for electrochemical luminescence (ECL), as well as other applications. It can also be embedded in other analytical devices for example inlet or outlet of a high performance liquid chromatography (HPLC).

BRIEF DESCRIPTION OF THE DRAWINGS

[0047] Embodiments of the present disclosure will now be described, by way of example only, with reference to the attached Figures, wherein:

[0048] Figure 1 is a schematic view of a complete electrochemical flow cell in accordance with one embodiment of the present disclosure;

[0049] Figures 2A and 2B are schematic side view representations of flow-by and jet-flow type flow cell electrode configurations of the prior art;

[0050] Figure 2C is a schematic side view representation of a flow-through type electrode in accordance with an embodiment of the present disclosure, for use in the electrochemical flow cell of Figure 1;

[0051] Figure 3A is a partial top plan view of the electrode of Figure 2C;

[0052] Figure 3B is a partial cross-sectional view of the electrode of Fig. 2C, showing flow velocity though the electrode and the flow cell;

[0053] Figure 4A-4B are voltammogram graphs showing the results of voltammetry analysis conducted in 1 mM FcMeOH (ferrocene methanol) and 0.1 M KCl at a scan rate of 100 mV s^{-1} for a number of different flow rates through the electrode of Fig. 2C and the flow cell of Figure 1;

[0054] Figure 5A is a voltammogram graphs showing the results of voltammetry analysis conducted for flow through the electrode of Fig. 2C and the flow cell of Figure 1, wherein current response was measured for different concentrations of $K_4Fe(II)CN_6$ in solution at a constant flow rate of 6mL min^{-1};

[0055] Figure 5B is a graph of current (in mA) vs. concentration (in mM), showing the anodic peak versus the concentration of $K_4Fe(II)CN_6$ in solution;

[0056] Figure 5C depicts the electrochemiluminescence (ECL) signal measurements obtained from the flow cell of Figure 1 over time, for 1 mM Tris(bipyridine)ruthenium(II) with 0.2 M of the co-reactant tripropylamine (TPrA) dissolved in 0.1 M phosphate buffer pH 7.3;

[0057] Figure 6 depicts a schematic representation of a method of manufacturing ultramicroelectrodes (UMEs) in accordance with an embodiment of the disclosure;

[0058] Figure 7 depicts optical micrographs for various disk UMEs formed with different electrode materials according to the method of Figure 6;

[0059] Figure 8A depicts steady-state voltammograms for UMEs of different electrode materials manufactured according to the method of Figure 6;

[0060] Figure 8B depicts negative and positive feedback approach curves for UMEs of different electrode materials as manufactured according to the method of Figure 6;

[0061] Figure 9 depicts optical micrographs of a mercury disk UME after electrodeposition and mechanical polishing manufactured according to an embodiment of the invention together with negative and positive feedback approach curves for said mercury disk UME;

[0062] Figure 10 depicts optical micrographs of $Ag/AgCl$ a microreference electrode manufactured according to an $Ag/AgCl$ embodiment of the invention together with steady-state voltammograms for 10 different microreference electrodes;

[0063] Figure 11 depicts a mercury deposition curve according to an embodiment of the invention together with linear sweep voltammetry results;

[0064] Figure 12 depicts steady-state voltammograms for bare disk electroactive surface UMEs and for Hg hemisphere UMEs with a Hg hemisphere deposited on the surface exploiting Pt, Au, Ag and C with insets of optical micrographs with a scale bar of 25 μm;

[0065] Figure 13 depicts optical micrographs of a burst 25 μm silver UME together with the same UME after a quick re-polish together with steady-state voltammograms for both the burst and the re-polished 25 μm Ag disk UMEs as manufactured using processes according to embodiments of the invention; and

[0066] Figure 14 depicts exemplary UMEs according to embodiments of the invention with multiple electrodes.

DETAILED DESCRIPTION

ELECTROCHEMICAL FLOW CELL

[0067] Referring to Figure 1, the electrochemical flow cell 10 (or simply "flow cell") of the present disclosure is a modular cell which enables scaling the device as may be

required and also permits modulation of the cell output signal without a substantial loss in reproducibility and accuracy. This is at least partially enabled by maintaining laminar flow though in the cell 10, as will be seen. By sustaining laminar flow through the cell, the flow cell 10 may enable improved predictability of the output signal and a better match between the actual signal output and the theoretical output which can be calculated using theory.

[0068] In comparison with the "flow-by" and "jet-flow" type flow cell electrode configurations of the prior art (see Figures 2A and 2B, respectively), the present flow cell 10 and thus the electrodes 12 therein employ a "flow-through" type configuration as shown in Fig. 2C. In this flow-through configuration, the fluid (e.g. reactant) flows through the cell 10, from an inlet 13 to an outlet 15 thereof, by serially flowing through each of the electrodes 12 in succession.

[0069] As seen in Figure 1, the flow cell 10 includes a cell body 20 having the inlet 13, the outlet 15, and a flow passage 22 defined by and within the cell body 20 and extending between the inlet 13 and the outlet 15 to define a flow path 17 for fluid flowing through the cell body 20. A number of electrodes 12 are disposed within the flow passage 22 of the cell body 20. Each of these electrodes 12 is a flow-through type electrode having an electrode surface 19 disposed transverse (and in at least one embodiment, substantially perpendicularly) to a flow direction 17 through the flow passage 22. In order to permit flow therethrough, the flow-through electrodes 12 have a plurality of apertures or other suitable openings or fluid flow passages or conduits therein through which the fluid can pass. The electrodes 12 are arranged in serial flow succession within the flow passage 22, such flow entering the cell body 20 via its inlet 13 must first flow through an upstream working electrode 14, before flowing to an intermediate counter electrode 16 and then, in turn, to a most downstream reference electrode 18. Fluid flow exiting the reference electrode 18 then flow toward the outlet 15 of the flow body 20. In the exemplary embodiment, therefore, the flow-through electrodes 12 include an upstream working electrode 14 at which the electrochemical reaction occurs, an intermediate counter electrode 16 which is used to

pass current density between the working electrode 14 and a downstream reference electrode 18 having a fixed potential. These three electrodes are disposed sequentially and in serial flow within the flow passage of the cell body. The working electrode 14 is disposed closest to the inlet 13 of the cell, the reference electrode 18 is disposed closest to the outlet 15 of the cell, and the counter electrode 16 is disposed between the upstream working electrode 14 and the downstream reference electrode 18.

[0070] As shown in Figure 1, at least the working electrode 14 and the counter electrode 16 may be honeycomb flow-through electrodes, as will be described. The reference electrode 18 may be formed by a small wire and a thin film.

[0071] The most upstream one of the electrodes 12 within the flow cell 10, namely the working electrode 14, therefore receives substantially un-interrupted fluid flow from the inlet 13 of the cell. In at least one embodiment, the working electrode 14 is positioned within the flow passage 22 at a predetermined distance Le downstream of the inlet 13 of the cell body 20. This predetermined distance or length Le is selected such as to corresponding to a streamwise location within the flow passage 22 at which substantially fully developed laminar flow of the fluid flowing along the flow path 17 occurs. This distance Le will vary depending on a number of factors, mainly the Reynolds Number of the fluid in question and the diameter D (or cross-sectional area for a non-circular cell flow passage) of the flow passage 22, however given these known parameters one skilled in the art will be able to accurately determine the point at which substantially fully developed laminar flow will occur given the particular conditions and parameters of the flow cell 10, the overall flow system in general and its intended use.

[0072] The distance Le of the working electrode 14 downstream of the inlet 13 of the flow cell 10 corresponds to the fluid dynamic "entrance effect" of flow through a pipe (or in this case, the flow passage 22 of the cell body 20). Boundary layers develop along the walls of the flow passage 22 as a result of the solid surface exerting a retarding shear force on the flow which reduces the speed of the flow near the walls.

As the distance Le away from the inlet 13 of the passage 22 increases, the effect of the passage wall is "felt" further out into the flow. The flow in this region is said to be developing. At a given point away from the passage inlet or entrance 13, the boundary layers developing on the walls reach the center line of the passage, at which point the shape of the velocity profile no longer changes with any increasing distance. This point is commonly called the "entrance length" (Le), after which the flow is said to be fully developed. The entrance length (Le) is therefore the length of pipe or cell flow passage 22 required for the flow to become fully developed. The entrance length (Le) is a function of the diameter (D) of the passage 22 and the Reynolds Number (Re), as follows:

$$Le/D \approx 0.06(Re).$$

[0073] The Reynolds number (Re) is a dimensionless diameter which determines the nature of the flow regime (i.e.: laminar or turbulent) for incompressible fluid flow in a pipe/channel. For fluid flow in a pipe, Reynolds numbers less that about 2300 indicate laminar flow, and Reynolds number greater than about 4000 indicate turbulent flow. A Reynolds number between these values indicates that the flow is transitional. Reynolds number is calculated as follows:

$$Re = \rho VD/\mu$$

wherein ρ is density, V is velocity, D is pipe diameter, and μ is dynamic viscosity. Thus, it will be understood that the transition between laminar flow and transitional flow is determined by the transition Reynolds number (Re^T), which is approximately equal to 2300.

[0074] Further, while the fluid flow reaching the working electrode 14 is therefore intended to be as laminar as possible, the fluid flow through the entire flow length of the cell 10, that is from at least the working electrode 14 to the outlet 15 of the flow passage, may also be kept as laminar as possible. This is possible given the relative lack of flow disturbances in the flow cell 10 and the flow-through nature of each of the electrodes 12, which will be described in further detail below.

[0075] Under such laminar flow conditions, the flow-through configuration of the electrodes 12 and the cell 10 offers several benefits over the flow by and jet-flow systems of the prior art, as seen in Figures 2A-2B. In the flow-by system of Figure 2A, only reactant that can diffuse to the plane of the electrode will undergo electrolysis. In the jet-flow configuration of Figure 2B, the radial flow gives a change in solution velocity across the electrode which may create stagnation points in the fluid flow, which may reduce temporal resolution for injection style analytical studies.

[0076] In contrast, by adopting the flow-through configuration of the present electrodes 12 and flow cell 10, as shown in Figure 1 and 2C, a substantially uniform and predictable hydrodynamic profile over the surfaces of the electrodes 12 (and particularly the surface of the working electrode 14) is provided, and a relatively short electrode length may also be used. Because laminar flow through the flow cell 10 may thus be enabled, improved predictability and reproducibility for the cell signal may be possible. The flow cell 10 so composed may also enable the simultaneous acquisition of a number of parameters, such as absorbance and electrochemiluminescence (ECL) for example. Any electrical interference and resistance that would otherwise arise from a more complicated electrode arrangement or problematic geometry between the working and the counter electrodes may therefore be reduced. Furthermore the reference electrode is downstream in order to minimize any possible contaminations.

[0077] In a particular embodiment, the electrodes 12, and particularly the working electrode 14, are honeycomb screen-printed electrodes. As can be seen in Figure 3C, the honeycomb configuration of the electrodes 12 define an electrode surface 19 that is symmetrical about a six planes of planes of symmetry extending through corners of the hexagonal shaped honeycomb electrode surface and through the central point of each edge of the hexagon. In Fig. 3A (see the insert), two exemplary planes of symmetry are shown. It is however to be understood that fewer or more planes of symmetry may alternately be provided. For example, two planes of symmetry that are perpendicular to each other are possible, both with the hexagonal shape of the

honeycomb configuration and/or with alternate electrode shapes. Regardless of the planes of symmetry, a substantially uniform electrode surface 19 extends across the entire flow passage 22 of the cell. The honeycomb electrodes 19 define a plurality of individual passages 24 which extend between the upstream electrode surface 19 and a downstream surface of the electrode 12. These passages 24 which extend in the flow-wise direction through the electrode therefore permit the fluid to flow through the electrodes 12.

[0078] As can be seen in Figure 3B, which shows simulated flow results for the fluid flow velocity through the honeycomb electrodes 12, the disturbance in the laminar flow through these electrodes is relatively minimal, and therefore the flow-through honeycomb electrodes 12 are not believed to cause undue disturbance to the overall laminar flow through the flow passage 22 of the cell body 20.

[0079] The hydrodynamic profile within the cell was also investigated by the inventors using finite element simulations using commercial software (Comsol Multiphysics 5.0). Calculations solved the Navier-Stokes equations for incompressible laminar fluid flow. As can be seen in Figure 3B, the velocity profile of the electrodes is shown. Here, solution enters the simulated domain, through the inlet at a velocity derived from the volume flow rate. The solution passes through a honeycomb electrode, before proceeding through the remainder of the device (not shown). Prior to the honeycomb electrode the flow is laminar, upon entrance to the honeycomb structure the flow accelerates through the individual tubules, before emerging. Flow after the honeycomb electrode returns to laminar after a short entry length. The simulation shows that the fluid flow provides well defined convection.

[0080] To empirically examine the flow cell 10 and the electrodes 12 used therein, the inventors performed cyclic voltammetry (CV) measurements, the results of which are shown in Figures 4A-5C.

[0081] A solution of 1 mM FcMeOH (ferrocene methanol) in 0.1 M KCl was pumped through the cell 10 at different flow rates while the electrochemical response was

measured. As the flow rate increased the measured current response increased, as shown in Figure 4A. Additionally, a change in the shape of the voltammogram from a peaked response to a steady-state plateau due to the increasing contribution of convection to the mass transport can be observed when the flow rate is greater than 5 mL min^{-1} through the device. Each measurement was repeated three times. Figure 4B shows the results recorded at 1 mL min^{-1} where the reproducibility of the measurement is clearly demonstrated.

[0082] Further, in order to confirm the analytical capabilities of the flow cell 10, the current response for different concentrations of $K_4Fe(II)CN_6$ at a constant flow rate were measured. Figure 5A shows the raise in the anodic current with the increase in the $K_4Fe(II)CN_6$ concentration. When plotting the anodic peak versus the concentration of $K_4Fe(II)CN_6$, as shown in Figure 5B, a linear fit ($R^2 = 0.9992$) was obtained providing an excellent calibration curve for analytical concentration measurements.

[0083] To demonstrate the versatility of the design of the flow cell 10, measurements for the electrochemiluminescence (ECL) signal of Tris(bipyridine)ruthenium(II) (referred to as Ru(bpy)) were also obtained. In this example, a solution of 1 mM Ru(bpy) and 0.2 M of the co-reactant tripropylamine (TPrA) dissolved in 0.1 M phosphate buffer pH 7.3 was pumped through the device at different flow rates, including tests conducted at 2 mL min^{-1} and 4 mL min^{-1}. The ECL signal was measured under hydrodynamic control and while a CV was performed, and the ECL signal was clearly measured as shown in Figure 5C. The strength of the ECL signal may also be dependent on the flow rate. This may be of particular interest, as the presently described flow cell 10 may thus provide a hydrodynamic ECL device, which may enable a number of commercially useful applications.

[0084] Accordingly, the modular flow-through cell 10 of the present disclosure is capable of performing both qualitative and quantitative measurements, and is further able to perform ECL measurements. The flow cell 10 may therefore be able to be

used in a variety of different research fields, ranging from fundamental studies, such as those relating to reaction mechanisms for example, to applied analysis, such as for sensing biological, organic and inorganic compounds for example. Furthermore, the flow cell 10 may also be scaled up and used in different industrial process or for on-line environmental monitoring, for example only.

[0085] The flow cell 10 may therefore offer several improvements over the existing commercially available systems, and may be used for a number of different applications. The flow cell 10 uses a flow-through methodology to obtain a reliable hydrodynamic profile, which may also dramatically increases the mass transport and increases the sensitivity of the detection while at the same time improving the signal to noise (S/N) ratio. The flow cell 10 can incorporate electrodes composed of different materials (such as: Au; Pt; and glassy carbon), and allow collection efficiency measurements for the study of homogenous kinetics, or the measurement of a generated species stability. Generally, the design of flow cell 10 can be adjusted for different purposes, thereby making it possible to increase the range of applications from a scientific and commercial point of view. The design of the flow cell 10 of the present disclosure can also be further miniaturized, in order to make it usable for applications such as in-field measurements such as environmental monitors and remote sensors. Additionally, as noted above, the flow cell 10 is able to perform ECL measurements, which provides significant possibilities.

ULTRAMICROELECTRODE

[0086] The electrochemical flow cell 10 as described above includes a number of electrodes 12. Because of the very small size of such flow cells 10, and therefore of the electrodes used therein, in order to provide predictable and accurate results, reproducibility and manufacturability considerations of the electrodes 12 become important. Because of their microscopic size, it has been found that improvement may also be sought with respect to the ability to consistently and accurately produce

the electrodes 12 in general, and the working electrodes 14 in particular given that this is where the electrochemical reaction occurs.

[0087] An improved method of manufacturing an ultramicroelectrode (or "UME") will now be described. These UMEs may be adapted, in one particular embodiment, for use in or as the working electrode 14 of the flow cell 10 as described above. However, the UMEs as described herein may also be adapted for other uses, and therefore it is to be understood that the presently described UMEs can be used as stand alone devices, and need not necessary be used in conjunction with an electrochemical flow cell. For example, such UMEs may be used in scanning electrochemical microscopy (SECM) applications or other applications in electrochemistry that involve imaging. Further, the UMEs as produced in accordance with the present disclose may also be used for conducting electrochemical measurements in low conductive media (such as organic solvents, etc.), where the voltage drop associated with high solution resistance makes such experiments difficult for conventional electrodes.

[0088] UMEs may be defined as electrodes with at least one dimension smaller than $25\mu m$. UMEs permit a very small voltage drop, which leads to a very small voltage distortion at the electrode-solution interface. This may permit, for example, using a two-electrode setup in voltammetric experiments, instead of a more conventional three-electrode setup. Apart from their small dimensions they may offer several advantages including, for example, high sensitivity, fast steady state response, low double-layer charging currents, high scan rates and small ohmic losses. Furthermore, their small current requirements enable electrochemical measurements in low conductive media, e.g. organic solvents, where the voltage drop associated with high solution resistance makes these experiments difficult for convention electrodes.

[0089] UMEs with small RG are also used in scanning electrochemical microscopy (SECM), in order to reduce tip-to-substrate distance (d) and thus allowing for a higher sensitivity.

[0090] The RG of a UME is defined as the ratio between the radius of the insulating sheath (r_T) and the radius of electroactive surface (a). The RG also has a significant effect on the current recorded during SECM approach curve measurements. A smaller RG will result in a larger current at short tip-to-substrate distances (<5) because of enhanced contributions from back diffusion of the mediator. They also decrease the probability of contact between the insulating sheath of the UME and the sample, which experimentally occurs upon axial misalignment of the UME.

[0091] Common geometries of such UMEs include disk, hemispherical, inlaid ring, ring-disk, and finite conical. The most frequently used geometry for UMEs is disk, whereby an electroactive material is embedded within an outer insulating layer. UMEs have been used in a variety of applications including biological systems, charge transport at liquid/liquid interfaces, and corrosion studies.

[0092] As noted above, the fabrication of high quality UMEs with a controlled geometry is a difficult and time-consuming process, which requires experimental skill and patience. A critical geometric parameter affecting the overall quality of the UME is the RG.

[0093] Accordingly, the inventors have developed an improved method of manufacturing such UMEs, in order to address at least some of these reproducibility and fabrication issues known to exist with existing UMEs.

[0094] The UMEs are produced in accordance with the method of fabrication(s) as will be described below have been found to be precisely reproducible with accurate geometries. This therefore enables exact quantitative analysis given the highly reproducible geometries of the electroactive area and the surrounding glass. Better control of the diffusion field around the electrode may thus be possible, enabling the quantification of very low levels of analytes.

A: EXAMPLE(S)

[0095] Although one particular example of a method of fabricating UMEs in accordance with the present disclosure is provided below, it is to be understood that the specific example provided is but exemplary.

A.1: Materials and Reagents.

[0096] For gold and platinum UMEs the inventors started with 0.01mm and 0.025 mm diameter wire of purity 99.99% and hard temper. For silver UMEs silver wire of 0.025mm diameter and purity 99.99% was employed together with 0.011mm diameter carbon fiber (Tex, 720; filaments, 4000; grade, P25). Additionally, 0.007mm carbon wire was employed. To form the outer body of the UMEs the inventors employed as a starting material soda-lime glass capillaries with inner diameter / outer diameter $0.4267 \pm 0.05mm / 1.0 \pm 0.05mm$ and borosilicate capillaries $1.16mm / 2.0mm$. Abrasive polishing discs (4000 grit), alumina powder (0.05, 0.1, 0.3, and 1.0 μm particle diameter), electrically conductive silver loaded epoxy, 0.50 mm diameter copper wire, and gold connector pins were also employed.

A2: Equipment.

[0097] The UMEs were fabricated using a P-2000 laser-based micropipette puller system (Sutter Instruments), a PC-10-CA vertical pipette puller (Narishige) and a vacuum pump. The electroactive surfaces were exposed and polished using a Tegrapol 23 variable speed grinder / polisher. All electrochemical measurements were performed using an Electrochemical Probe Scanner 3 (HEKA Elektronik) in a three-electrode setup with a platinum wire counter electrode. All potentials were recorded relative to a chloridized silver wire quasi-reference electrode, unless specified otherwise, which had been manufactured at McGill University. Optical micrographs were obtained using a customized Axio Vert.A1 inverted microscope.

A3: Preparation of Solid Electrode Disk UMEs.

[0098] Referring to Figure 6, a complete schematic of the disk UME fabrication technique according to an embodiment of the present disclosure is presented. The

soda-lime glass capillary were cleaned using 10% v/v nitric acid for 1-2 hours, rinsed with nanopure water, and dried in an oven ($100°C$) for 12 hours, first stage 110. Then using the P-2000 micropipette puller, a capillary was pulled using a single line heating and pulling program (Heat: 240; Fil: 5; Vel: 60; Del: I40; Pul: 70), at the second stage 120. Equal tensile force was applied at each end of the capillary along with simultaneous heat from a CO_2 laser, resulting in the severing of the narrowed neck and thus production of two symmetric micropipette tips, as shown at the third stage 130.

[0099] Subsequently, a 10 mm long section of electroactive material in wire or fiber form, for example silver (Ag), gold (Au), carbon (C), or platinum (Pt), was inserted into the pulled micropipette tip. By placing the assembly tip down and applying gentle vibratory on the open extremity of the micropipette tip, the wire/fiber traveled downward until trapped in the sealed extremity. The assembly was then inserted into a PC-I0-CA vertical pipette puller, fourth stage 140, and a vacuum pump was attached to the open end of the micropipette, and the pressure was reduced for approximately 5 minutes to minimize bubble formation. The wire was sealed by centering the assembly inside a Kanthal heating coil and applying heat for $\sim 10-20s$ after maximum temperature was reached (bright orange coil), fifth stage 150. The sealed wire was connected to a copper (Cu) wire using conductive silver epoxy, which was subsequently cured at $120°C$ for 15 minutes. The assembly was inserted into a larger borosilicate capillary to provide additional reinforcement, and the overlapping edges were sealed using epoxy. A gold connector pin was then soldered to the copper wire, completing the assembly, sixth stage 160. The electroactive surface of the UME was exposed using a grinder/polisher (400 rpm, 4000 grit) followed by an alumina powder polishing.

[00100] According, as can be appreciated from the above and as depicted in Figure 6, a pre-thinning step 120 of the outer glass capillary is performed, prior to severing the thinned neck region. Because of the equal forces applied to the capillary

in opposite directions, the thinned neck region is formed having at least a very symmetric geometry, if not perfect symmetry. This has to be done to the glass capillary without the wire in place therewithin. Consequently, a high concentricity between the electroactive wire (whether formed of metal or fiber), once it is subsequently inserted into the capillary after this pre-thinning step, is achieved. This enables a very precise ratio of the amount of exposed electroactive wire tip to the surrounding glass sheath of the capillary. Or alternately stated, a very precise RG value of the UME so produced, which is the ratio between the radius of the insulating glass sheath (r_T) and the radius of electroactive wire tip (a). In one particular embodiment, this ratio RG is less than 10, and in a further particular embodiment the ratio RG obtained is about 3. In one particular embodiment, the resulting ultramicroelectrode so formed does not require any additional side polishing, after the sealing of the electroactive wire within the narrowed neck of the pulled capillary.

A4: Preparation of Mercury Electrode Disk UMEs.

[00101] Hg UMEs offer an extended solvent window in the negative potential region and an increase of sensitivity compared to Pt. In order to fabricate these, a post fabrication sequence was performed upon Au disk UMEs with an Au disk diameter of $25\mu m$. These were initially chemically etched by immersion in aqua regia (nitro-hydrochloric acid) solution for $10-20\,\text{min}$. The Au UME was then rinsed with acetone and nanopure water to halt etching. Hg was then electrodeposited onto the recessed electroactive surface of the UME using the same procedure as for Hg hemispherical UMEs described below in Section A6.

[00102] However, the potential was applied for a longer period of time, such that a Hg hemisphere protruded from the glass. A disk was then formed by mechanically polishing the excess Hg. Disk UMEs were stored in a degassed, 0.5% acidified 0.1 M KNO_3 solution.

A5: Preparation of Silver—Silver Chloride Microreference Electrodes.

[00103] Bare $25\mu m$ Ag disk UMEs were coated with silver chloride by immersion in a 1.0 M KCl solution with the application of 2.0 V in a two-electrode setup using a Pt wire counter electrode for $20s$ according to the reaction given in Equation (1). The microreference electrodes were stored in 0.1 M KCl when not in use.

$$AgCl_{(s)} + e^- \leftrightarrow Ag_{(s)} + Cl^-_{(s)} \qquad (1)$$

A6. Preparation of Hg Hemispherical UMEs

[00104] Hg hemispherical UMEs, with Ag, Au, C, or Pt, were fabricated by electrodeposition according to the reaction given in Equation (2). Briefly, an Hg hemisphere was electrodeposited onto the electroactive surface of a disk UME using 10 mM $Hg_2(NO_3)_2$ in 0.1 M KNO_3 acidified to 0.5% with HNO_3 solution. The electrochemically-controlled deposition was performed by applying a potential of -0.5 V vs. $Hg/HgSO_4$ until the current reached π/2 (~1.57) times the initial current from the $25\mu m$ disk UME. The Hg deposition curve is shown Figure 6A wherein a potential of $0V$ was held for 0.35 seconds before a potential step of -0.5 V vs. $Hg/HgSO_4$ (saturated K_2SO_4) was applied for a duration of 300 seconds. The full coverage of the electroactive surface has been investigated for both Hg disk and hemispherical UMEs. Similar to the Hg disk UME, see Figure 6B, the hemispherical UMEs display the expected shift in proton reduction to more negative potentials compared to the bare disk UMEs. Once fabricated, the Hg hemispherical UMEs were stored in degassed, 0.5% acidified 0.1 M KNO_3 solution.

$$Hg_2^{2+}(aq) + 2e^- \leftrightarrow 2Hg(l) \qquad (2)$$

A6. Electrochemical Measurements.

[00105] Electrochemical behavior was characterized by cyclic voltammetry and SECM approach curves. Ferrocenemethanol ($FcMeOH$; 1 mM) was used for Au, C, and Pt measurements, while hexaammineruthenium(III) chloride (ruhex;

$Ru(NH_3)_6Cl_3$; 1 mM) was used for measurements with Ag and Hg. For cyclic voltammetry using $FcMeOH$, the potential was varied linearly from -100 mV to +400 mV, while a window of 0 mV to -500 mV versus Ag was used with ruhex. All cyclic voltammograms (CVs) were performed using a scan rate of $10mV \cdot s^{-1}$.

[00106] SECM approach curves were performed at constant potential of $400mV$ for $FcMeOH$ and $-400mV$ for ruhex ($-450mV$ vs. Ag for Hg). Negative feedback approaches were performed over solvent-resistant chlorotrifluoroethylene (CTFE) plastic, while positive feedback approach curves were performed over a $1.6mm$ gold disk macroelectrode. The speed of approach used was $1\mu m \cdot s^{-1}$.

B: RESULTS AND DISCUSSION

B1. Disk UME Characterization.

[00107] The fabrication procedure depicted and described in respect of Figure 1 was tested by 10 subjects without any prior electrode fabrication experience whatsoever, yielding consistently high quality UMEs. Whilst already shorter than prior art manufacturing approaches the fabrication process has several steps that can be performed concurrently for several UMEs (e.g., epoxy curing), allowing for batch production even with a manually based process in a research environment. Improved tooling, automation, etc. may further lower effective time per UME and accordingly their cost. Fabricated UMEs were characterized using optical microscopy, cyclic voltammetry, and SECM approach curves. These three complementary techniques evaluate several important parameters, including the RG, quality of the polishing and sealing, and most importantly, the electrochemical behavior of the UME.

[00108] Side view images of fabricated UMEs such as depicted in first to seventh image sets 200A to 200G in Figure 7 for UMEs confirm the absence of air bubbles and a proper concentric seal of the wire/fiber within the insulating glass sheath. First to seventh image sets representing:

[00109] First image set 200A depicts a $10\mu m$ Pt UME;

[00110] Second image set 200B depicts a $25\mu m$ Pt UME;

[00111] Third image set 200C depicts a $10\mu m$ Au UME;

[00112] Fourth image set 200D depicts a $25\mu m$ Au UME;

[00113] Fifth image set 200E depicts a $25\mu m$ Ag UME;

[00114] Sixth image set 200F depicts a $7\mu m$ C UME; and

[00115] Seventh image set 200G depicts a $11\mu m$ C UME.

[00116] The scale bar in each instance being 25 µm. The sealed length was generally $3-5mm$. To avoid capillary bending during sealing, concentric alignment of the UME within the heating coil and coil temperature ($\sim 720°C$) were rigorously controlled. Bending effects were more prevalent when using smaller diameter wires. End views of the UMEs in the right hand images of each of first to fourth image sets 200A to 200D respectively confirms ideal disk geometry with a well-centered electroactive core surrounded by an insulating sheath, requiring no further sharpening step as employed in prior art manufacturing techniques.

[00117] To characterize the electrochemical behavior of the UMEs, cyclic voltammetry (CV) was used yielding first to fourth graphs 300A to 300D in Figure 8A wherein:

[00118] First graph 300A depicts $25\mu m$ and $10\mu m$ Pt UMEs;

[00119] Second graph 300B depicts $25\mu m$ and $10\mu m$ Au UMEs;

[00120] Third graph 300C depicts a $25\mu m$ Ag UME; and

[00121] Fourth graph 300D depicts $7\mu m$ and $11\mu m$ C UME.

[00122] The CV plots in first, second and fourth graphs 300A, 300B and 300D in respect of Pt, Au, and C UMEs were performed using 1 mM $FcMeOH$ in 0.1 M

KCl with an $Ag/AgCl$ reference electrode whilst the Ag UME in third graph 300C in 1 mM $Ru(NH_6)^{3+}$ in 0.1 M KNO_3 with an AgQRE. Scan speed was $10mV \cdot s^{-1}$.

[00123] To further characterize the electrochemical behavior of the UMEs, negative and positive feedback approach curves were obtained yielding first to fourth graphs 300E to 300H in Figure 8B wherein:

[00124] First graph 300E depicts $25\mu m$ and $10\mu m$ Pt UMEs;

[00125] Second graph 300F depicts $25\mu m$ and $10\mu m$ Au UMEs;

[00126] Third graph 300G depicts a $25\mu m$ Ag UME; and

[00127] Fourth graph 300H depicts $7\mu m$ and $11\mu m$ C UME.

[00128] The CV plots in first, second and fourth graphs 300E, 300F and 300H in respect of Pt, Au, and C UMEs were performed using 1 mM $FcMeOH$ in 0.1 M KCl with an $Ag/AgCl$ reference electrode whilst the Ag UME in third graph 300G in 1 mM $Ru(NH_6)^{3+}$ in 0.1 M KNO_3 with an AgQRE. UMEs were approached at a speed of $1\mu m \cdot s^{-1}$.

[00129] The steady state current (i_{SS}) is governed by the flux of redox species in solution toward the electrode surface as described by Equation (3) where k is a geometric constant (disk, $k = 4$; hemispherical, $k = 2\pi$, n is the number of electrons involved in the reaction, F is the Faraday constant ($96{,}485C \cdot eq^{-1}$), a is the radius of the electroactive surface, D is the diffusion coefficient of the redox species ($D_{FcMeOH} = 7.8\times10^{-6}cm^2s^{-1}$; $D_{Ruhex} = 8.7\times10^{-6}cm^2s^{-1}$), $C*$ is the concentration of dissolved redox species, and β is a tabulated factor dependent on the RG of the UME.

$$i_{SS} = k \cdot n \cdot F \cdot a \cdot D \cdot C* \cdot \beta \qquad (3)$$

[00130] Using Equation (3) and the experimental i_{SS} of the CVs presented in Table 1 then the diameters of the electroactive surface of the UMEs were calculated, as reported above the corresponding CVs are depicted in first to fourth graphs 300A to 300D in Figure 8B. The calculated diameters are consistent with those observed in optical micrographs (first to seventh image sets 200A to 200G respectively in Figure 7) and reported by the manufacturer of the respective wire/fiber, confirming a high quality seal devoid of leaks and cracks, which would have manifested as an increased steady state current. This seal quality is further confirmed by the presence of a long current plateau over hundreds of millivolts. The lack of significant hysteresis in the CVs is also qualitatively indicative of a good polishing.

Electroactive Surface	Electroactive Surface Diameter (μm)	RG	Steady State Current (nA)	n
Carbon	7	3.2 ± 0.1	1.07 ± 0.0003	4
	11	2.5 ± 0.1	1.64 ± 0.02	3
Gold	10	3.2 ± 0.2	1.51 ± 0.02	4
	25	2.7 ± 0.1	3.78 ± 0.04	5
Platinum	10	3.6 ± 0.1	1.51 ± 0.02	5
	25	2.7 ± 0.1	3.70 ± 0.05	5
Silver	25	2.7 ± 0.2	-4.47 ± 0.21	4
Average	---	3.0 ± 0.2	---	30

Table 1: RG of Experimental Disk UMEs

[00131] SECM approach curves were used to determine RG. UMEs were approached toward an insulating or conducting surface while biased at a constant potential, producing negative and positive feedback currents, respectively (see second image 300B in Figure 8A). The RG can be determined by fitting the experimental

approach curves to theoretical expressions for current over an insulator or conductor. The RG of fabricated disk UMEs are tabulated in Table 1 above. Using the proposed technique, UMEs with small RG are readily achievable. Moreover, the results in Table 1 indicate that the geometry of the fabricated UMEs is reproducible across electrode materials, with an average $RG = 3.0 \pm 0.2$ for $n = 30$ samples. The data is presented as mean ± standard error of the mean. The number of data points is defined as n. In comparison to a non-exhaustive compilation of commercially available SECM-grade disk UMEs, currently available commercial disk UMEs are typically much larger than the ones reported in Table 1, and may for example be between 100 and 300. The UMEs reported herein exploiting lower complexity, higher yield manufacturing processes are comparable to the best commercial UMEs.

B2. Mercury Disk UME Characterization.

[00132] Hg disk UMEs were fabricated using a combination of chemical etching, electrodeposition, and mechanical polishing. Optical micro- graphs were obtained at different stages of the fabrication process. The side view image, first image 400A in Figure 4 highlights a chemically recessed Au UME. Etching depth can be adjusted by controlling the immersion time in aqua regia. Since the bare disk UMEs used during this fabrication process were previously characterized, it was determined that the diameter of the produced gap was equal to the diameter of the electroactive core (i.e., using a $25\mu m$ Au disk UME, the diameter of the gap was also $25\mu m$). Following Hg electrodeposition and mechanical polishing, the side image (second image 400B in Figure 9) and top (third image 400C in Figure 9) views of the optical micrographs confirm the disk geometry of the Hg UME. The top view depicted in third image 400C in Figure 9 also demonstrates that the Hg electroactive area is well-centered within the glass sheath.

[00133] Subsequently Hg disk UMEs were characterized using CV (first graph 400D in Figure 9) and SECM approach curves (second graph 400E in Figure 9). Again, using Equation (3) and the i_{SS} from the CV (first graph 400D in Figure 9), the

diameter of the Hg disk UME was $25\mu m$, which is consistent with the diameter of the recessed Au wire backbone. The positive and negative feedback approach curves (second graph 400E in Figure 9) were fitted to theoretical expressions. The behavior of the Hg disk UME was equivalent to its Au disk UME backbone, with the same RG. The complete surface coverage of the Hg on the recessed gold surface was demonstrated using linear sweep voltammetry as depicted in Figure 11, whereby a $650mV$ overpotential cathodic shift in the proton reduction current is observed at the Hg UME as compared to the recessed disk UME. The development of Hg disk UMEs allows for an extended solvent window in the negative potential region, which is not possible with conventional cores such as Au or Pt, and also offers an increase of sensitivity compared to other metals for the electroanalysis of trace metal. Moreover the disk geometry allows fitting to established theoretical expressions. The method can also produce Hg hemispherical UMEs as description supra in respect of Section A6.

B3. Silver—Silver Chloride Microreference Electrode Characterization.

[00134] Top and side view optical micrographs are presented in first and second images 500A and 500B in Figure 10 wherein an $AgCl$ layer has successfully been electrodeposited onto the bare Ag disk UME. In order to evaluate the electrochemical stability of the microreference electrodes, cyclic voltammetry in $FcMeOH$ was employed. Referring to graph 500C in Figure 10 there are depicted cyclic voltammograms obtained with 10 different microreference electrodes and the same working electrode ($25\mu m$ Pt disk UME). The exhibited electrochemical behavior is consistent with the response obtained from a commercial (and much larger) reference electrodes. Even after 100 cycles, electrochemical response remained stable. The experimental E^0 was calculated to be $166.9 \pm 2.3mV$ ($n = 10$). The small size of these microreference electrodes make them suitable for use in microelectrochemistry.

B4. Mercury Disk UME Characterization.

[00135] The electrochemical behavior of Hg hemispherical UMEs was characterized using cyclic voltammetry from -300 mV to -900 mV versus Hg/Hg_2SO_4 and is depicted in Figure 12 with first to fourth graphs 700A to 700D respectively wherein:

[00136] First graph 700A depicts $25\mu m$ Pt disk UME and Hg/Pt UMEs with insert side view optical micrograph;

[00137] Second graph 700B depicts $10\mu m$ Au disk UME and Hg/Au UMEs with insert side view optical micrograph;

[00138] Third graph 700C depicts $25\mu m$ Ag disk UME and Hg/Ag UMEs with insert side view optical micrograph; and

[00139] Fourth graph 700D depicts $11\mu m$ C disk UME and Hg/C UMEs with insert side view optical micrograph.

[00140] Lateral view optical micrographs, insets in first to fourth graphs 700A to 700D confirmed full surface coverage of the Hg hemisphere on the electroactive core (Ag, Au, C, or Pt) without expansion to the glass sheath, i.e. not overgrown, and determined that Hg hemispheres were properly tethered. All cyclic voltammetry were recorded in 1 mM $Ru(NH_3)_6Cl_3$ in 0.1 M KNO_3 at a scan rate of $10mV \cdot s^{-1}$. The full surface coverage of the Hg on the active material was characterized using linear sweep voltammetry (0 V to +2.5 V versus Hg/Hg_2SO_4) in a 0.1 M KNO_3 as depicted in Figure 11, whereby the proton reduction over potential shifted to more negative potentials compared to a bare disk UME. In this case, potentials were recorded relative to a chloride free Hg/Hg_2SO_4 (sat. K_2SO_4) reference electrode. The response of hemispherical Hg UMEs showed, as expected, steady-state currents that were larger for hemispherical Hg UMEs compared to bare disk UMEs. This behavior was the result of the change in geometry from disk to hemispherical, which according to Equation (3) results in a steady-state increase of π/2, see Equation (4).

The well-defined geometry of the disk UMEs used as a backbone allowed relatively simple modification of their electroactive surface and produced hemispherical UMEs with an equally well-defined geometry, which makes them highly suitable for SECM measurements.

$$\frac{i_{SS,Hemisphere}}{i_{SS,Disk}} = \frac{2\pi}{4} = \frac{\pi}{2} \approx 1.57 \quad (4)$$

B5. "Burst Effect" Silver Disk UME.

[00141] A particular challenge was encountered during the fabrication of silver disk UMEs. Among the noble metals used, silver has the lowest melting point, which means it is also the softest. Sealing glass around the silver wire was not a problem but polishing the UME tip proved to be more difficult than other electroactive cores. Typically, the tip is polished until the electroactive surface is exposed. In the described protocol, this is done using a speed of 400 rpm for approximately 15 minutes. Electrochemical characterization using CV showed that the fabricated silver disk UMEs had an electroactive core with a diameter much larger than $25\mu m$, see graph 800C in Figure 13, which seemed unreasonable considering the inserted wire was only $25\mu m$. Subsequent optical microscopy imaging showed that the surface of UME was not flat, resembling a "burst effect", whereby the metal seemed to burst out of the capillary, see first image set 800A in Figure 13. After re-polishing for a short period (~1 minute), the surface became clean and flat (Figure 11), similar to other electroactive cores used. It was determined that in fact, the "burst effect" was caused by polishing for an extended period of time. The friction produced by the speed and time of polishing caused the silver to soften and "burst" out of the glass sheath. This observation highlights the fact that although polishing is an important component of the fabrication process, great care must be taken to ensure proper UME geometry.

C. Multi-Core UME and UME with Integrated Silver/Silver Chloride Reference Electrode Fabrication

[00142] Within the descriptions supra in respect of Figure 6 through Figure 13, UMEs have been formed individually.

[00143] However, referring to Figure 14 there are depicted first and second schematics of variant methodologies wherein multiple wires or fibers can be sealed in the soft glass capillary to produce multi-core UMEs. Accordingly, within first schematic 900A a capillary has been exploited to form the UME with 5 electrical contacts. It would be evident that the metal within each contact may be different, the same, or different combinations may be employed. In second schematic 900B there is depicted a UME with an integrated silver/silver chloride reference electrode 910 in conjunction with a UME 920. Such an electrode is produced by a similar methodology as that described in respect of Section A3 but using a double-barrel soft glass capillary and then following this procedure the methodology described in Section A5 is applied to the silver core producing an UME with an integrated reference electrode. Accordingly, a combination may be formed such as that with first schematic 900A in Figure 14 such that the central electrode is a silver/ silver chloride reference and the outer electrodes are all gold, for example, or are gold, platinum, mercury and carbon in another embodiment or two carbon and two gold in yet another.

[00144] Accordingly, the inventors have demonstrated a general technique for the fabrication of disk UMEs with different electroactive cores, including carbon, gold, mercury, platinum, and silver. This technique leads to UMEs with small RG ranging from 2.5 to 3.6 although the inventors believe smaller RGs are possible. Beneficially, the fabrication technique reduces the time required, improves the ease of fabrication, provides controlled and reproducible geometry, and the ability to expand to multiple electroactive cores. Furthermore, the disk UMEs produced using this technique make them suitable backbones for surface modified electrodes, demonstrated here by the production of Hg disk, hemispherical UMEs, and Ag/AgCl microreference electrodes. Further, the optimal geometry of these probes makes them highly suitable for use in SECM measurements.

[00145] It would be evident that multi-core UMEs may be formed through combining multiple capillaries, exploiting a multi-bore capillary, or exploiting a machined or drilled glass block providing improved reproducibility of bore-bore tolerances.

[00146] The foregoing disclosure of the exemplary embodiments of the present invention has been presented for purposes of illustration and description. It is not intended to be exhaustive or to limit the invention to the precise forms disclosed. Many variations and modifications of the embodiments described herein will be apparent to one of ordinary skill in the art in light of the above disclosure. The scope of the invention is to be defined only by the claims appended hereto.

CLAIMS:

1. An electrochemical flow cell comprising:

a cell body having an inlet, an outlet, and a flow passage extending between the inlet and outlet to define a flow path for fluid flowing through the cell body;

a number of flow-through electrodes disposed within the cell body and in said flow passage, the flow path extending through said flow-through electrodes, which each have an electrode surface disposed transverse to a flow direction along the flow path through the flow passage, said flow-through electrodes arranged in serial flow succession within the flow passage and including at least an upstream working electrode, a downstream reference electrode, and a counter electrode disposed between the working electrode and the reference electrode, the flow-through electrodes having a plurality of apertures therein through which the fluid passes; and

wherein the working electrode is positioned within the flow passage at a predetermined distance downstream of the inlet of the cell body, said predetermined distance corresponding to a streamwise location at which substantially fully developed laminar flow of the fluid flowing along the flow path through the cell body.

2. The electrochemical flow cell of claim 1, wherein the flow passage is free of flow disturbances to generate substantially fully developed laminar flow throughout the flow passage of the flow cell, from at least the upstream working electrode and the outlet of the flow passage.

3. The electrochemical flow cell of claim 1 or 2, wherein the flow passage is substantially circular in cross-sectional shape and defines a diameter.

4. The electrochemical flow cell of claim 3, wherein said predetermined distance is an entrance length (Le) of the flow passage, wherein the entrance length (Le) is determined as: Le= 0.06 * Re * D, where Re is the Reynolds Number and D is the diameter of the circular flow passage.

5. The electrochemical flow cell of any one of claims 1 to 4, wherein the flow-through electrodes have flow-facing electrode surfaces that are symmetrical about two perpendicular planes of symmetry.

6. The electrochemical flow cell of claim 5, wherein the at least the working electrode and the counter electrode have honeycomb configurations.

7. The electrochemical flow cell of claim 6, wherein the working electrode and the counter electrode are honeycomb screen-printed electrodes.

8. The electrochemical flow cell of claim 6, wherein the honeycomb configurations of the working electrode and the counter electrode define a plurality of individual passages that extend in a direction of the flow path between the flow-facing electrode surfaces on an upstream side and a downstream surface on an opposite side of the flow-through electrodes, the individual passages providing substantially uninterrupted fluid flow therethrough.

9. The electrochemical flow cell of claim 1, wherein the electrode surfaces of said electrodes are disposed perpendicularly to the flow direction through the flow passage.

10. The electrochemical flow cell of any one of claims 1 to 9, wherein the flow cell is modular, permitting a number of said electrochemical flow cells to be interconnected with each other.

11. The electrochemical flow cell of any one of claims 1 to 10, wherein the electrochemical flow cell is operable to simultaneously acquire absorbance and electrochemiluminescence (ECL) measurements.

12. A hydrodynamic electrochemiluminescence (ECL) device comprising the electrochemical flow cell of any one of claims 1 to 10, wherein the electrochemical flow cell generates an electrochemiluminescence (ECL) signal.

13. A method of obtaining at least one of electrochemical and spectroscopic measurements from respective sensor, comprising connecting the electrochemical flow cell of any one of claims 1 to 10 to the respective sensor in electrical flow communication and generating a fluid flow through the electrochemical flow cell.

14. A flow system in connection with the electrochemical flow cell of any one of claims 1 to 10, further comprising a spectroscopic sensing module having a spectroscopic detector in communication with at least the working electrode.

15. A flow system in connection with the electrochemical flow cell of any one of claims 1 to 10, further comprising an electrochemical sensing module in communication with at least the working electrode, the electrochemical sensing module being configured to perform at least one of potentiometric, galvanostatic, and impedance based electrochemical measurements.

16. A method of manufacturing an ultramicroelectrode, comprising:

pulling a capillary according to a predetermined pulling profile, the predetermined pulling profile applying substantially equal tensile forces to each of the opposed ends of the capillary in opposite directions to form a narrowed neck in the capillary, the narrowed neck defining a capillary wall that is symmetrical relative to a longitudinal axis extending centrally through the capillary at the narrowed neck thereof;

severing the narrowed neck of the capillary to form two separate micropipette tips, each having an opening symmetrically defined within the capillary walls;

inserting an electroactive wire into the opening defined within the capillary wall of at least one of the tip ends formed from the pulled capillary; and

sealing the tip end having the electroactive wire inserted therein by applying heat to fuse the electroactive wire within the surrounding capillary walls.

17. The method of claim 16, wherein the step of severing the narrowed neck of the capillary includes at least one of applying the tensile forces until the capillary breaks at the narrowed neck and breaking the narrowed neck of the pulled capillary at predetermined position.

18. The method of claim 17, wherein breaking the narrowed neck further comprising applying local heat to the predetermined position heat using a laser.

19. The method of claim 16, further comprising forming the ultramicroelectrode to have a ratio of a radius of the capillary wall to a radius of the electroactive wire at the tip end of less than 10.

20. The method of claim 19, further comprising forming the ultramicroelectrode to have the ratio of the radius of the capillary wall to the radius of the electroactive wire at the tip end of from 2.5 to 3.6

21. The method of claim 20, further comprising forming the ultramicroelectrode to have the ratio of the radius of the capillary wall to the radius of the electroactive wire at the tip end of about 3.

22. The method of claim 16, wherein the step of sealing includes using a fusion process wherein a temperature based fusion of the capillary to the electroactive wire occurs.

23. The method of claim 16, further comprising selecting the electroactive wire to be one of a metal wire or a fiber wire.

24. The method of claim 16, further comprising severing the narrowed neck of the capillary at a substantial midpoint thereof.

25. A method of forming a multicore ultramicroelectrode using the method of any one of claims 16 to 24, wherein the capillary is a soft glass capillary, further comprising inserting multiple electroactive wires into the soft glass capillary after the steps of pulling and severing.

26. The method of claim 16, further comprising using electrodeposition on an exposed surface of the electroactive wire to form a hemispherical tip of the ultramicroelectrode.

27. The method of claim 16, further comprising providing the capillary with a plurality of bores extending therethrough.

28. A method of manufacturing a multicore ultramicroelectrode comprising:

pulling a double-barrel soft glass capillary of predetermined inner and outer diameters according to a predetermined pulling profile;

at least one of pulling until the capillary breaks at the reduced neck producing two pulled pipettes and breaking the pulled capillary at the reduced neck at predetermined position;

inserting a predetermined length of wire or fiber into one of the two compartment of the reduced neck of the pulled capillary and a predetermined length of a silver wire in the second one;

sealing the pulled capillary to the wire or the fiber and the silver wire via a predetermined fusion process;

exposing the electroactive surface of the UME; and

depositing silver chloride on the exposed silver disk.

29. The method according to claim 28, wherein the predetermined fusion process is a temperature based fusion of the capillary to the at least one of the wire and the fiber.

30. A method of manufacturing a multicore ultramicroelectrode comprising:

at least one of pulling and molding a glass preform having a predetermined outer geometry and a plurality of bores of predetermined inner diameters according to either a predetermined profile or a predetermined event occurs;

inserting a predetermined length of at least one of the wire and the fiber into at least one reduced bore of the plurality of bores; and

sealing the at least one reduced bore to the at least one of the wire and the fiber via a predetermined fusion process.

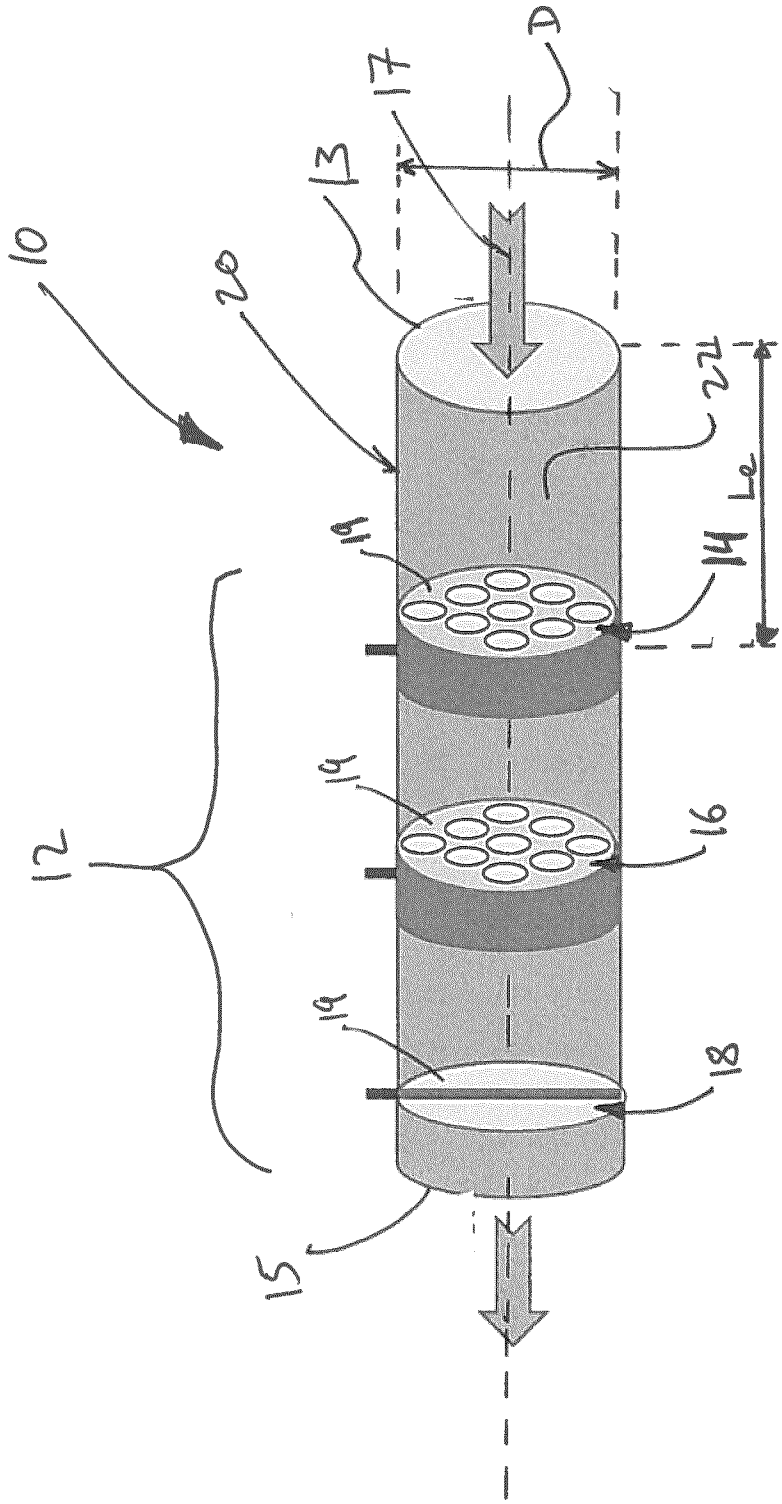

Figure 1

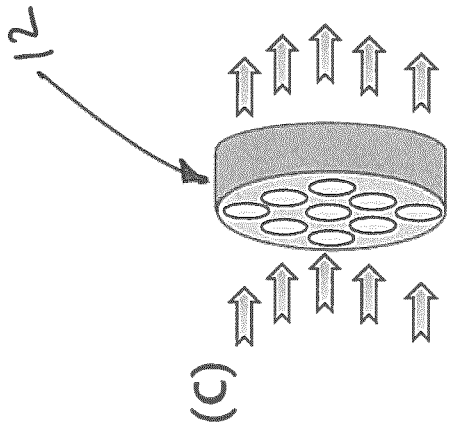

Figure 2C

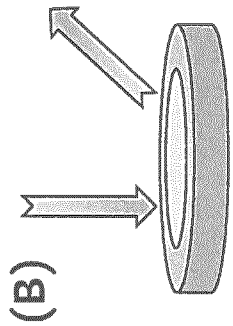

Figure 2B (prior art)

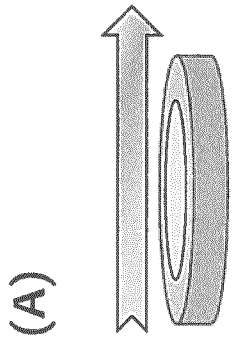

Figure 2A (prior art)

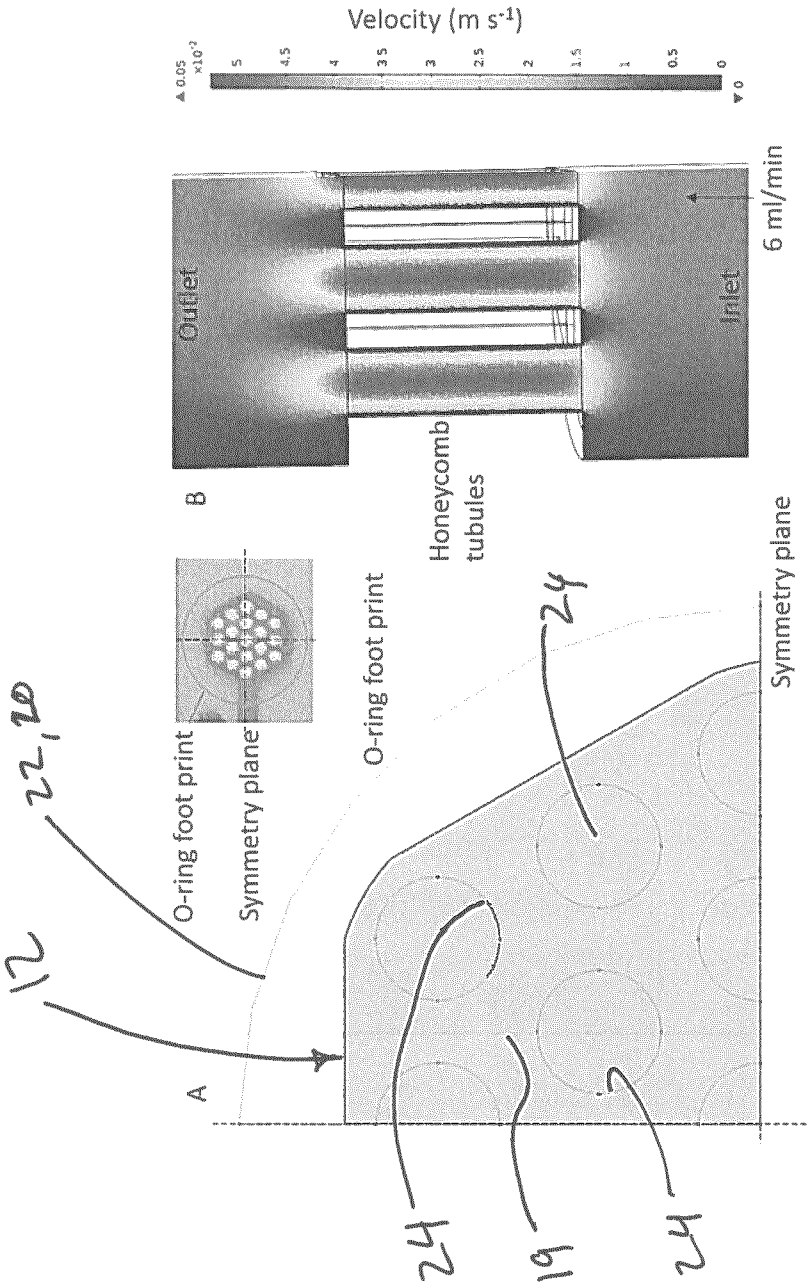

Figure 3A

Figure 3B

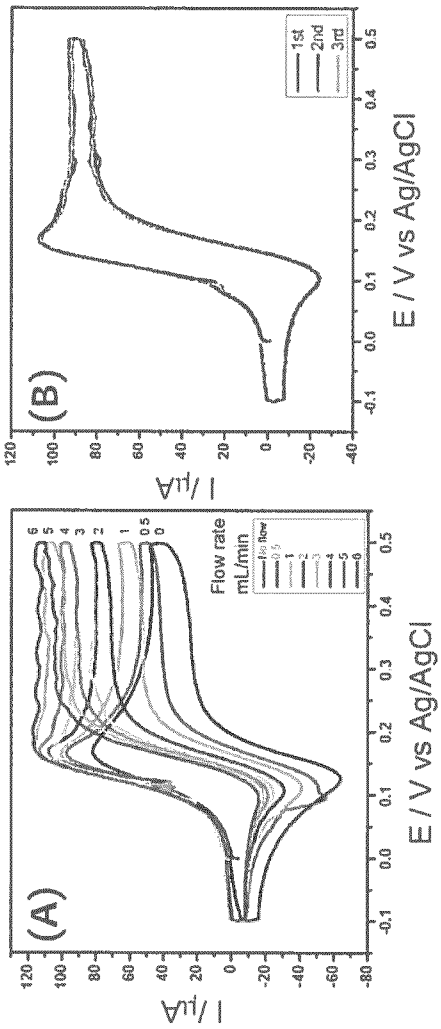

Figure 4A Figure 4B

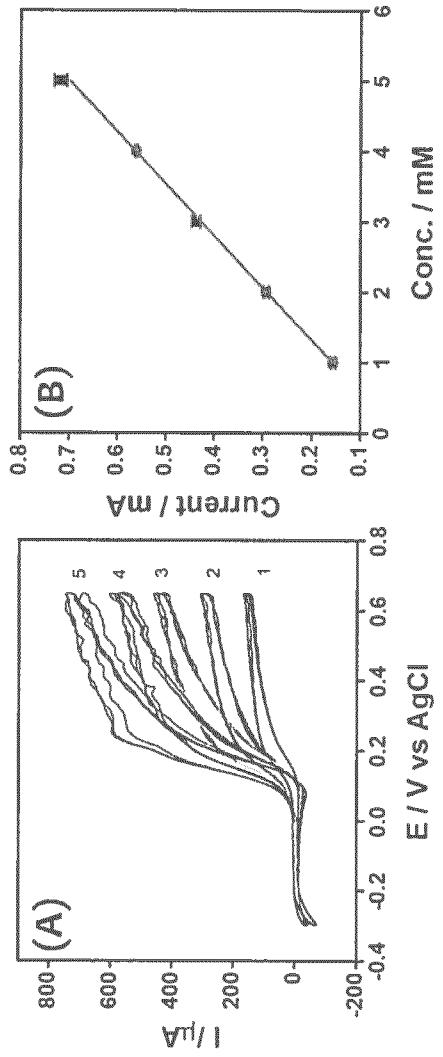

Figure 5A Figure 5B

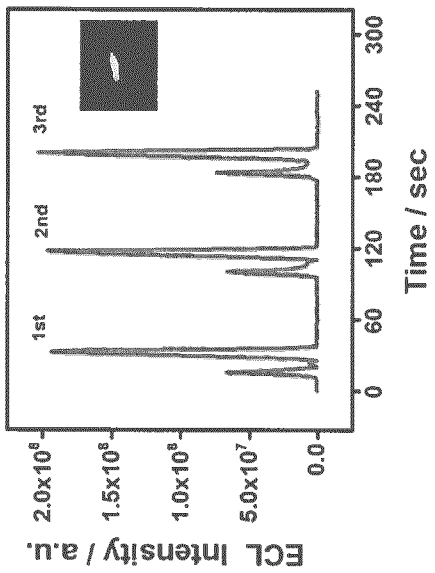
ECL Intensity / a.u.
2.0x10^8
1.5x10^8
1.0x10^8
5.0x10^7
0.0
0
60
120
180
240
300
Time / sec
1st
2nd
3rd

Figure 5C

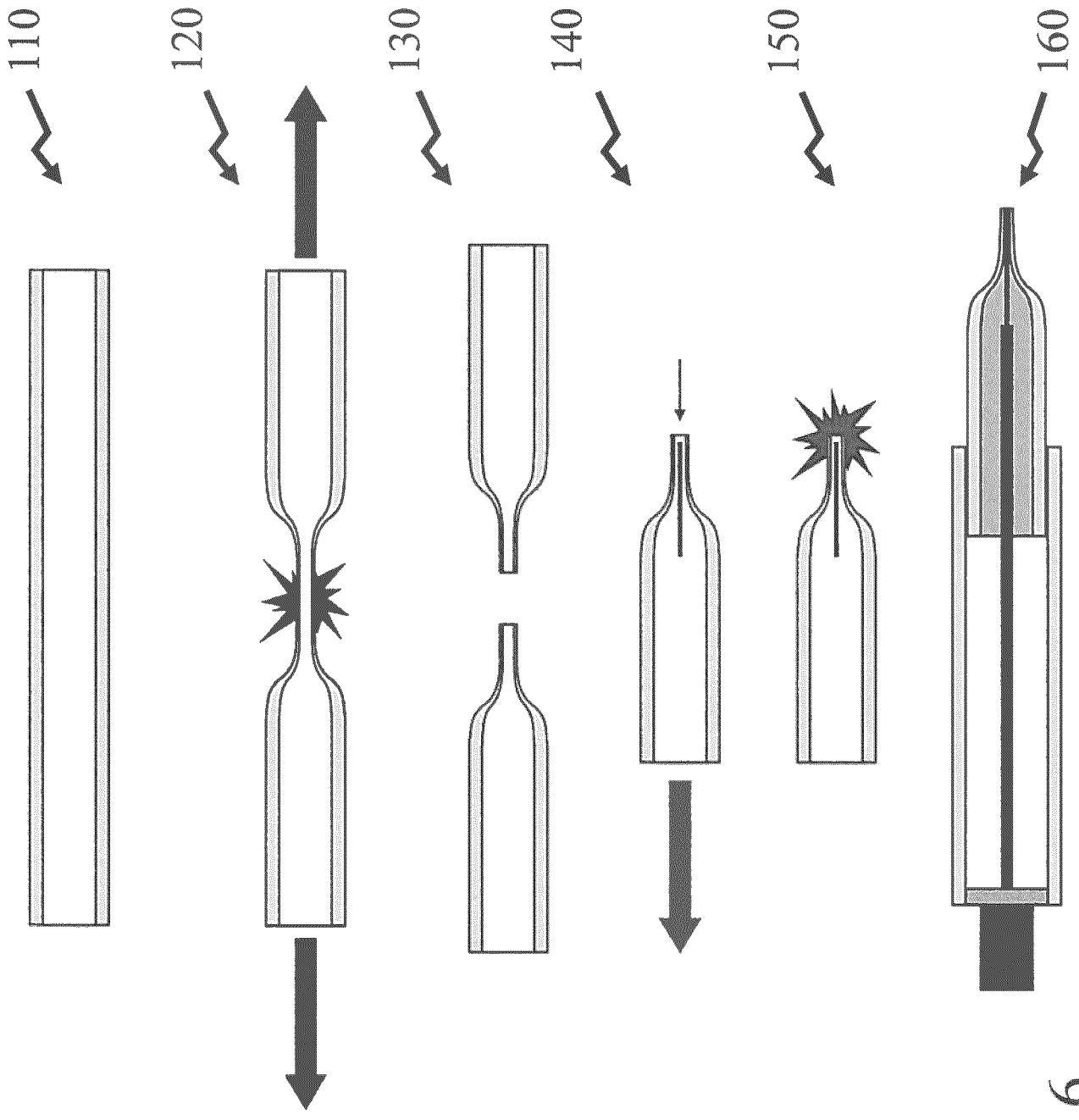

Figure 6

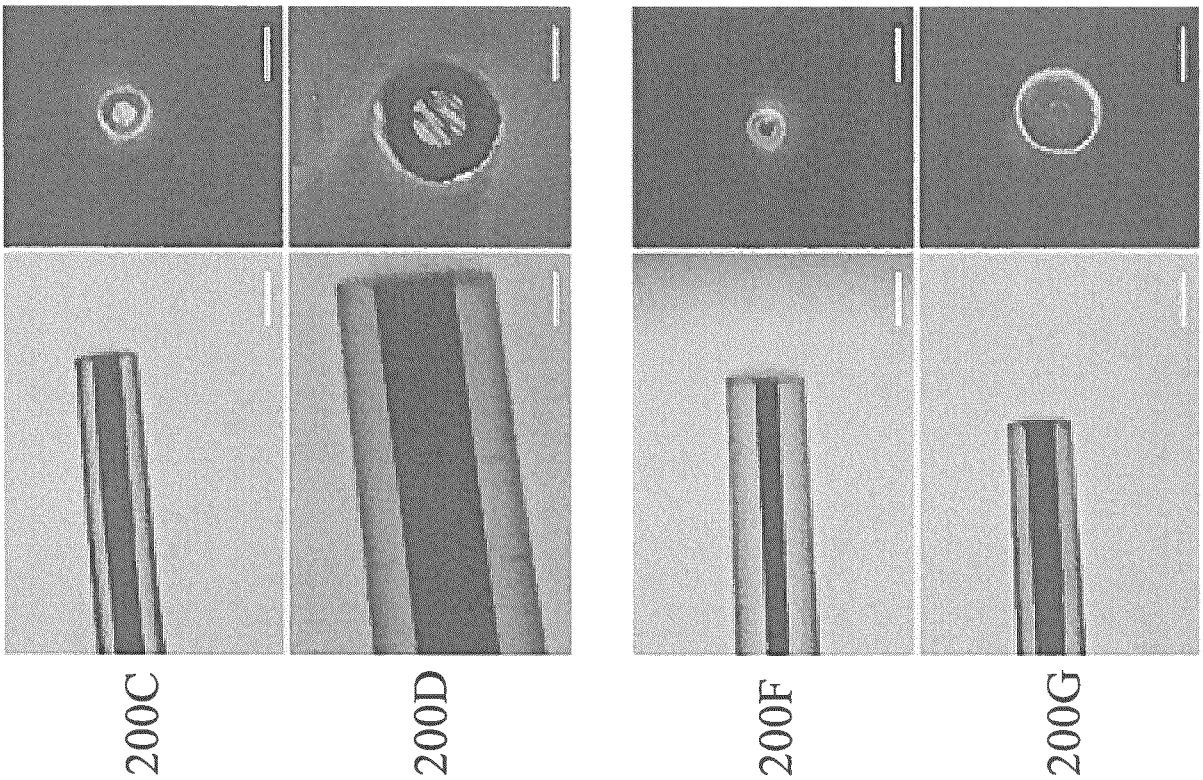

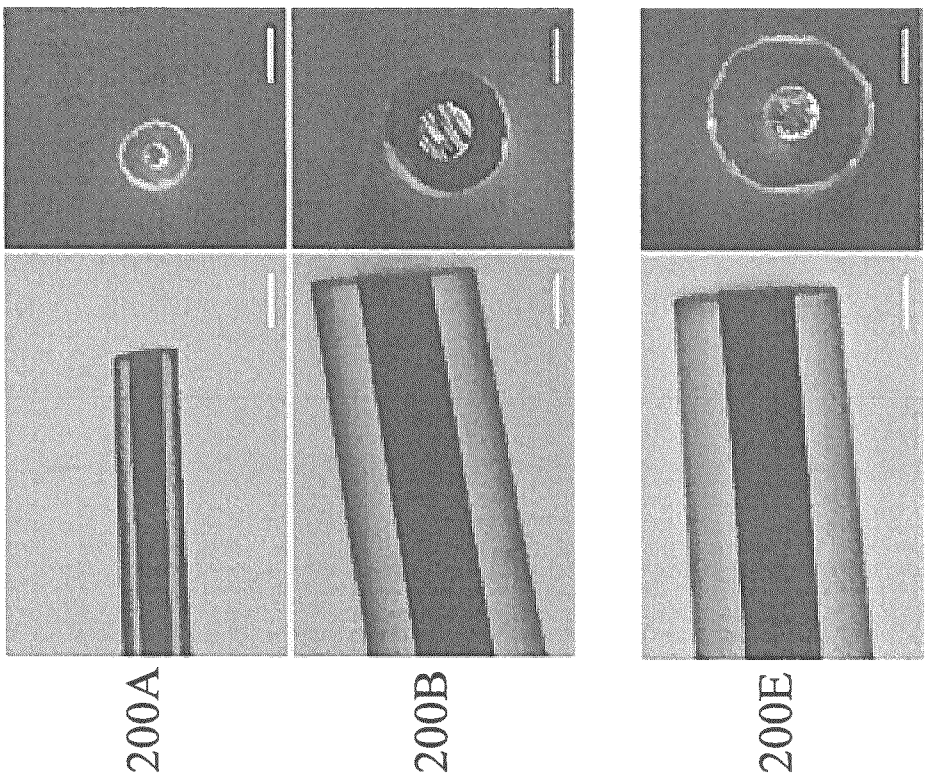

Figure 7

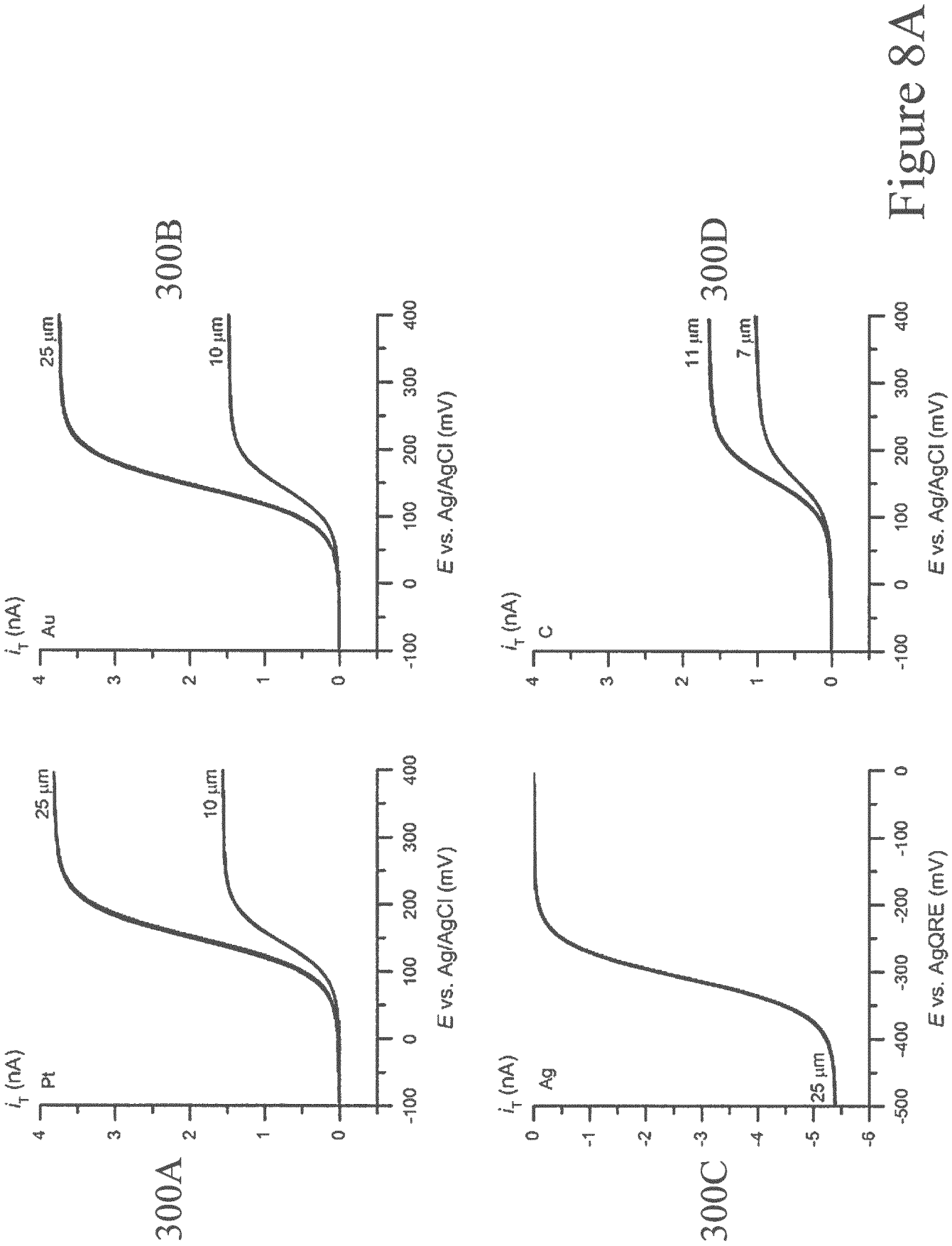
300A
Pt
25 µm
10 µm
i_T (nA)
E vs. Ag/AgCl (mV)
300B
Au
25 µm
10 µm
i_T (nA)
E vs. Ag/AgCl (mV)
300C
Ag
25 µm
i_T (nA)
E vs. AgQRE (mV)
300D
C
11 µm
7 µm
i_T (nA)
E vs. Ag/AgCl (mV)

Figure 8A

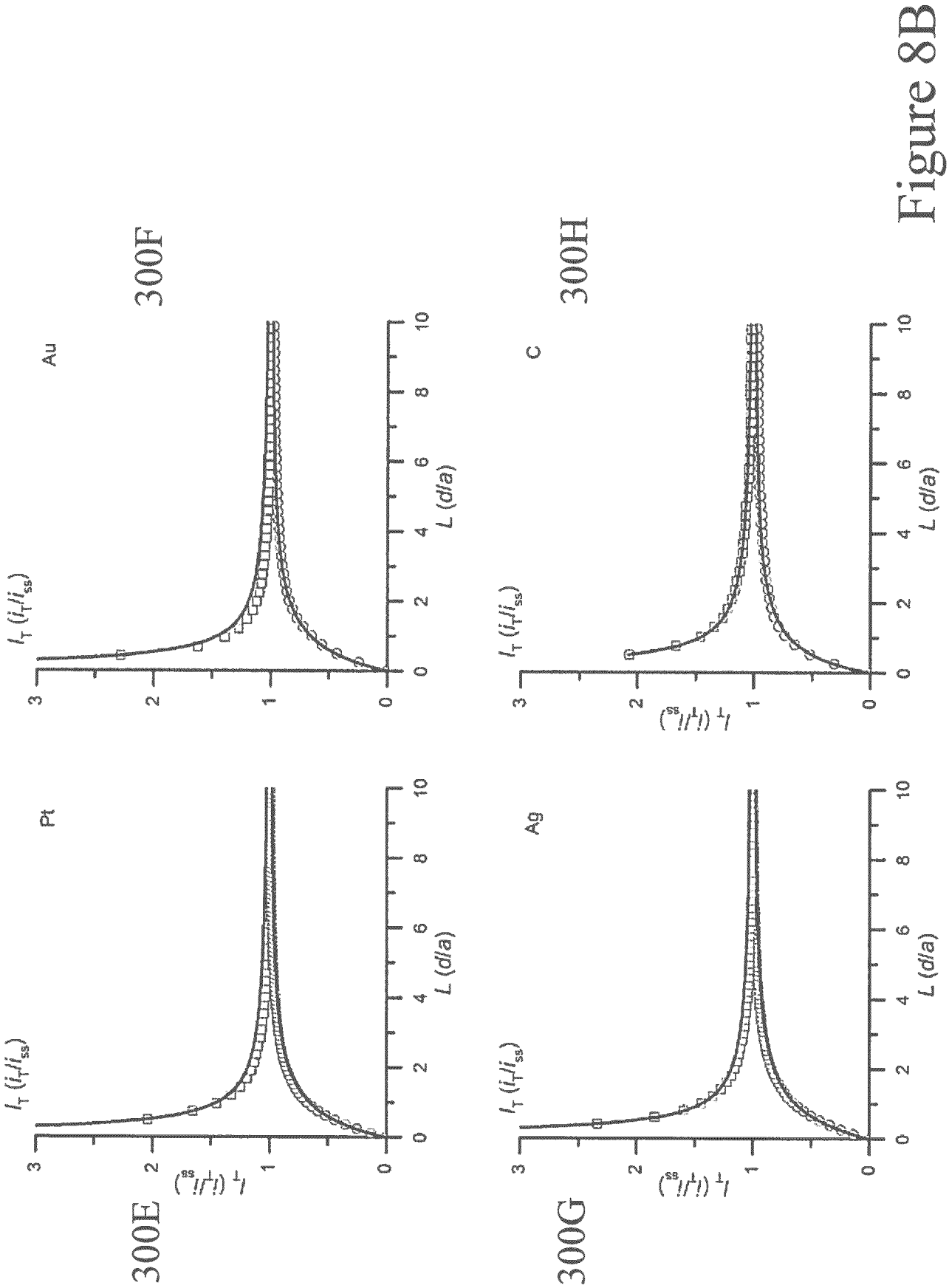
300E
Pt
300F
Au
300G
Ag
300H
C
I_T (i_T/i_{ss})
i_T (i_T/i_{ss})
L (d/a)
0
1
2
3
0
2
4
6
8
10

Figure 8B

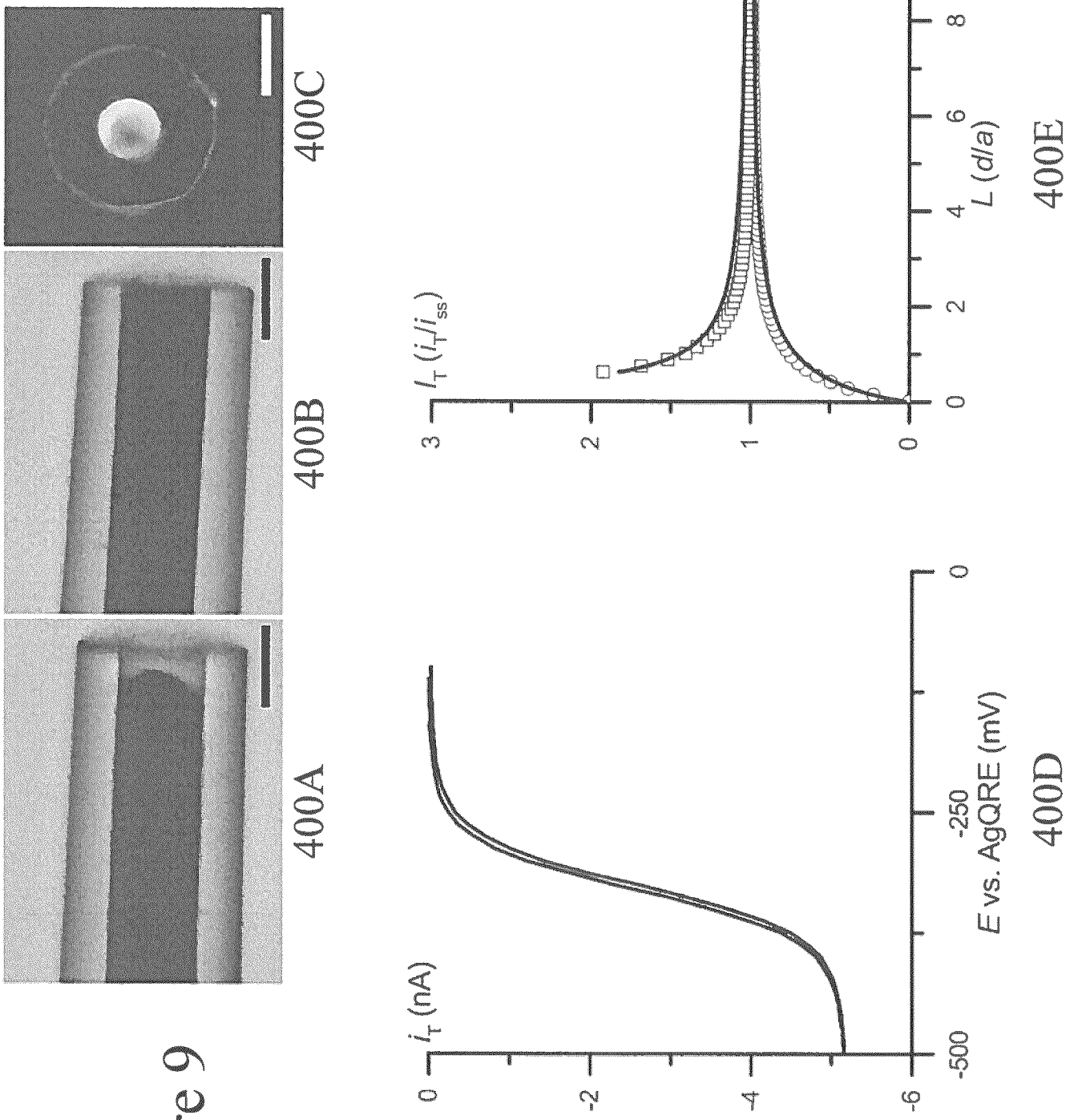
400A
400B
400C
400D
400E
i_T (nA)
0
-2
-4
-6
-500
-250
0
E vs. AgQRE (mV)
I_T (i_T/i_{ss})
3
2
1
0
0
2
4
6
8
10
L (d/a)

Figure 9

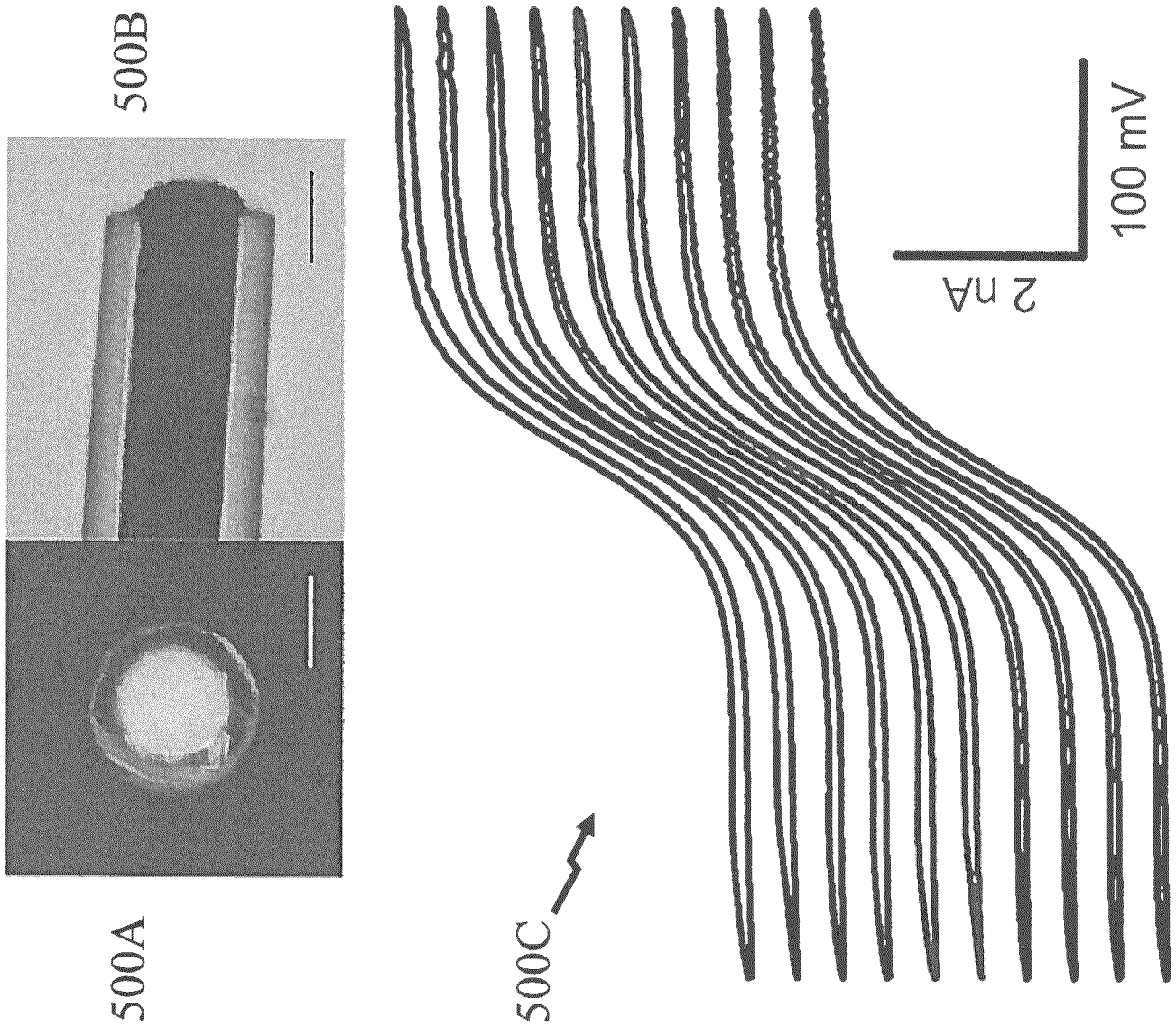

Figure 10

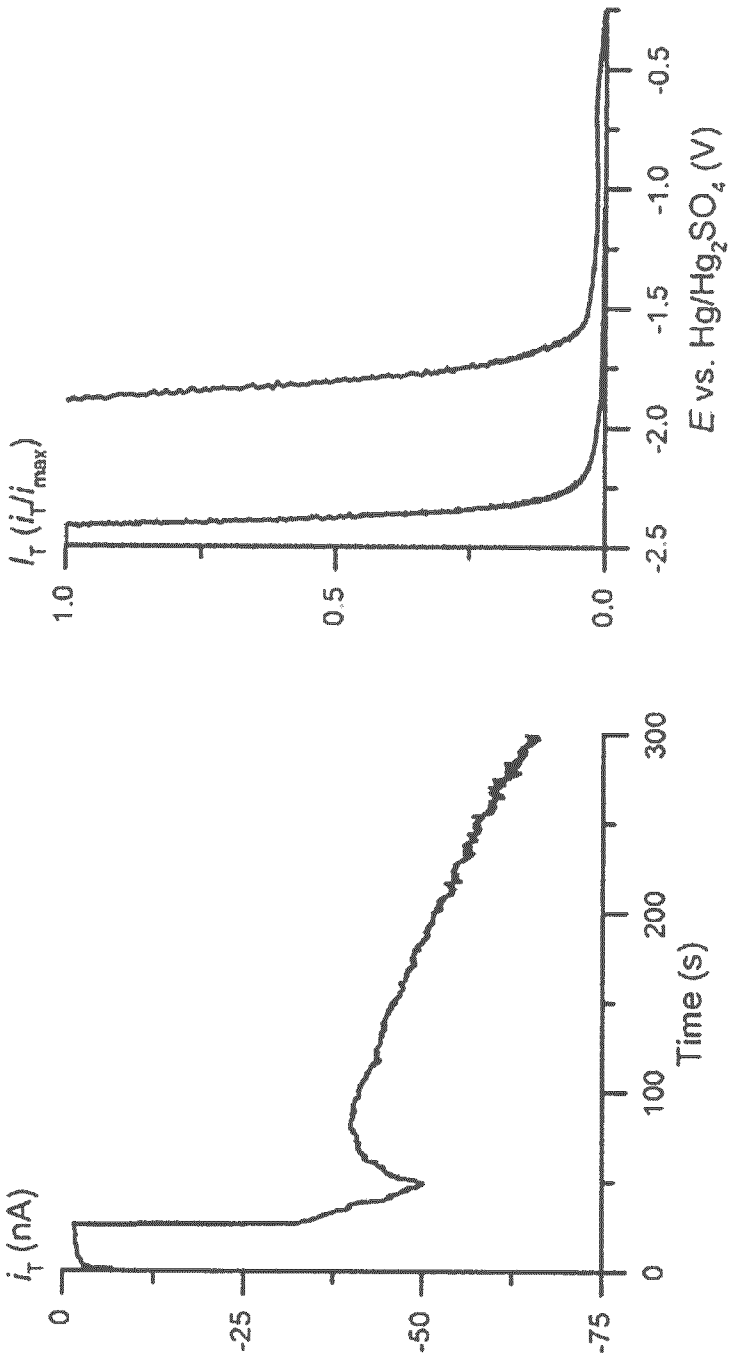
i_T (nA)
0
-25
-50
-75
0
100
200
300
Time (s)
600A
i_T (i_T/i_{max})
1.0
0.5
0.0
-2.5
-2.0
-1.5
-1.0
-0.5
E vs. Hg/Hg_2SO_4 (V)
600B

Figure 11

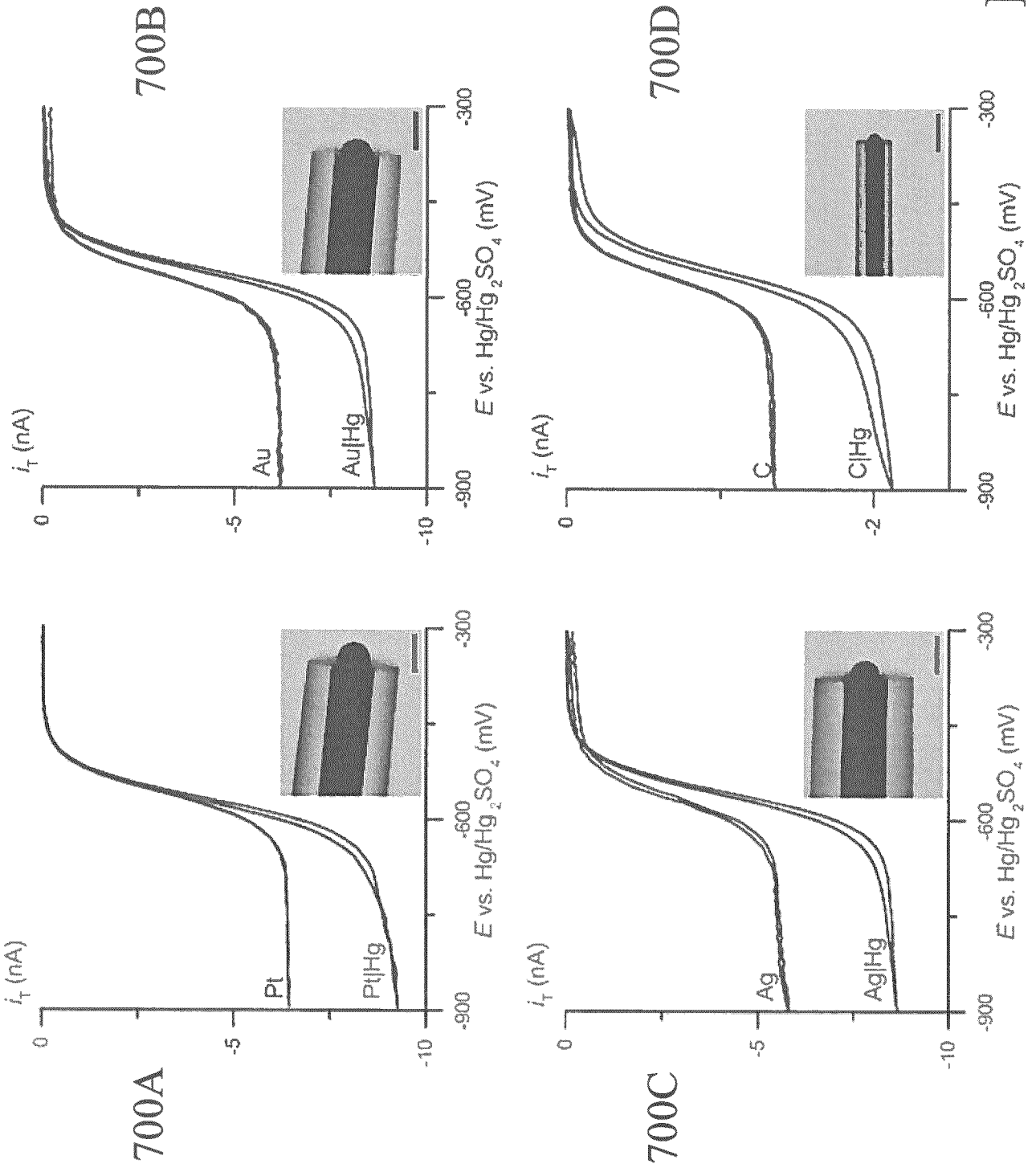
700A
700B
700C
700D
i_T (nA)
E vs. Hg/Hg$_2$SO$_4$ (mV)
Pt
Pt|Hg
Au
Au|Hg
Ag
Ag|Hg
C
C|Hg

Figure 12

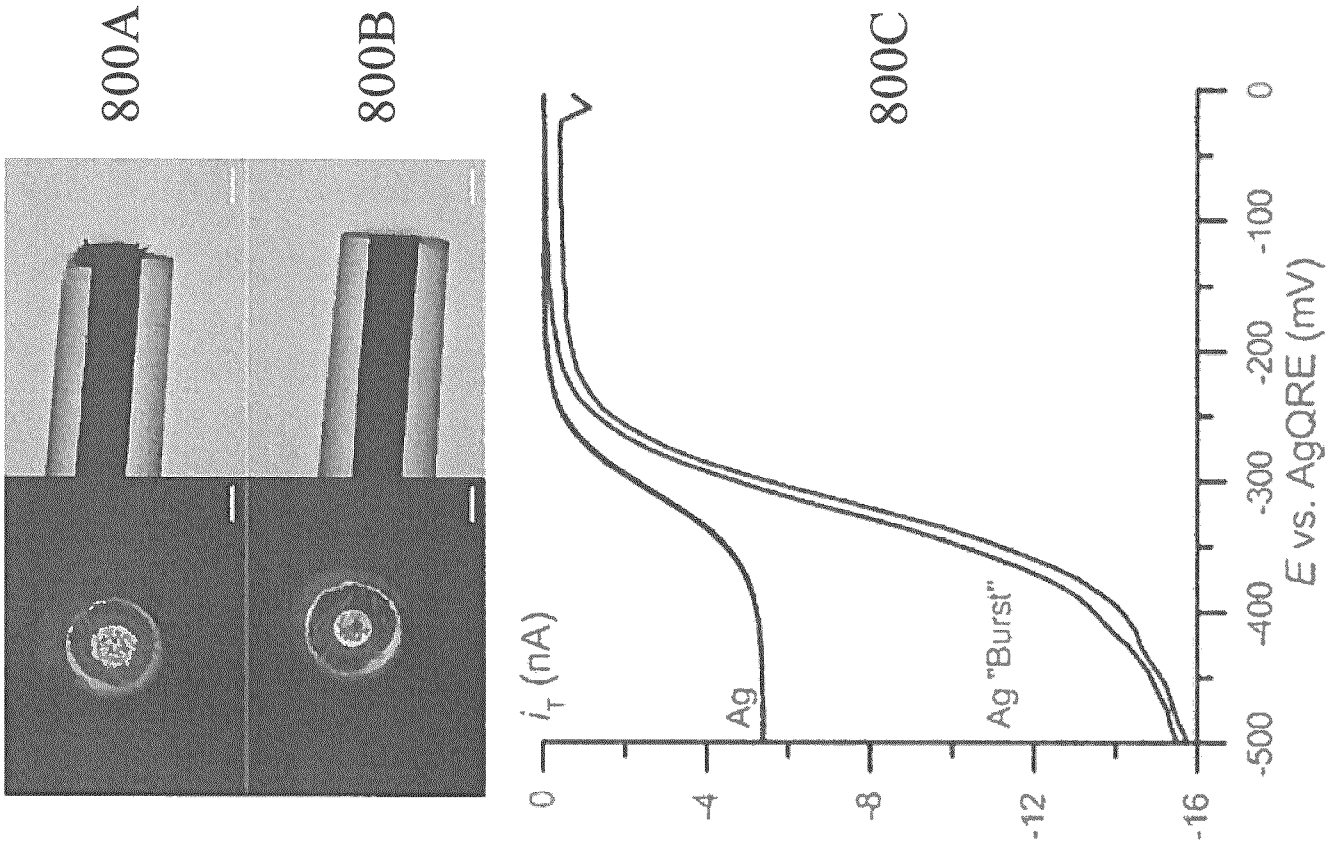
800A
800B
800C
i_T (nA)
0
-4
-8
-12
-16
Ag
Ag "Burst"
-500
-400
-300
-200
-100
0
E vs. AgQRE (mV)

Figure 13

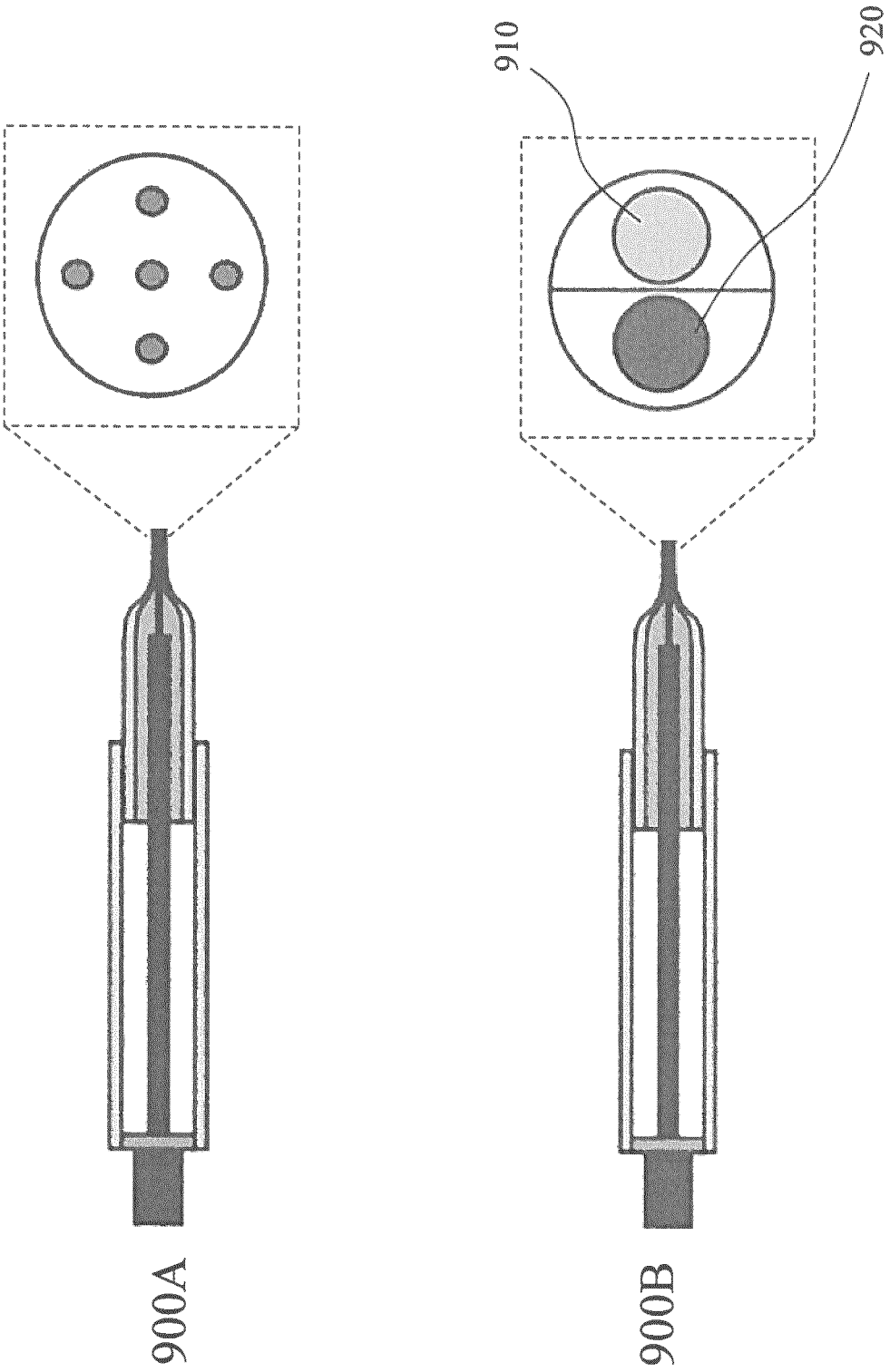

Figure 14

INTERNATIONAL SEARCH REPORT

International application No.
PCT/CA2016/050314

A. CLASSIFICATION OF SUBJECT MATTER
IPC: ***G01N 27/30*** (2006.01), ***G01N 21/66*** (2006.01), ***G01N 21/76*** (2006.01), ***G01N 27/36*** (2006.01), ***G01N 27/403*** (2006.01)

According to International Patent Classification (IPC) or to both national classification and IPC

B. FIELDS SEARCHED

Minimum documentation searched (classification system followed by classification symbols)
IPC: ***G01N 27/30*** (2006.01), ***G01N 21/66*** (2006.01), ***G01N 21/76*** (2006.01), ***G01N 27/36*** (2006.01),

Documentation searched other than minimum documentation to the extent that such documents are included in the fields searched

Electronic database(s) consulted during the international search (name of database(s) and, where practicable, search terms used)
Tools : Questel Orbit, Google, Canadian Patent Database, IEEE

Keywords: electrochemical, flow cell, laminar flow, electrode, manufacture, glass, capillary, pull, pipette

C. DOCUMENTS CONSIDERED TO BE RELEVANT

Category*	Citation of document, with indication, where appropriate, of the relevant passages	Relevant to claim No.
A	D1: US 5,911,859 15 June 1999 (15-06-1999) Greaney et al. ** See whole document **	1 to 15
A	D2: CN202542927 U 21 Novembre 2012 (21-11-2012) Wang et al. ** See whole document **	1 to 15
A	D3: US 2012/0006060 A1 12 January 2012 (12-01-2012) Terao ** See whole document **	16 to 30

☐ Further documents are listed in the continuation of Box C.

☑ See patent family annex.

*	Special categories of cited documents:
"A"	document defining the general state of the art which is not considered to be of particular relevance
"E"	earlier application or patent but published on or after the international filing date
"L"	document which may throw doubts on priority claim(s) or which is cited to establish the publication date of another citation or other special reason (as specified)
"O"	document referring to an oral disclosure, use, exhibition or other means
"P"	document published prior to the international filing date but later than the priority date claimed
"T"	later document published after the international filing date or priority date and not in conflict with the application but cited to understand the principle or theory underlying the invention
"X"	document of particular relevance; the claimed invention cannot be considered novel or cannot be considered to involve an inventive step when the document is taken alone
"Y"	document of particular relevance; the claimed invention cannot be considered to involve an inventive step when the document is combined with one or more other such documents, such combination being obvious to a person skilled in the art
"&"	document member of the same patent family

Date of the actual completion of the international search 27 May 2016 (27-05-2016)	Date of mailing of the international search report 31 May 2016 (31-05-2016)
Name and mailing address of the ISA/CA Canadian Intellectual Property Office Place du Portage I, C114 - 1st Floor, Box PCT 50 Victoria Street Gatineau, Quebec K1A 0C9 Facsimile No.: 819-953-2476	Authorized officer Francois Ziade (819) 576-2581

INTERNATIONAL SEARCH REPORT

International application No.
PCT/CA2016/050314

Box No. II Observations where certain claims were found unsearchable (Continuation of item 2 of the first sheet)

This international search report has not been established in respect of certain claims under Article 17(2)(a) for the following reasons:

1. ☐ Claim Nos.:
because they relate to subject matter not required to be searched by this Authority, namely:

2. ☐ Claim Nos.:
because they relate to parts of the international application that do not comply with the prescribed requirements to such an extent that no meaningful international search can be carried out, specifically:

3. ☐ Claim Nos.:
because they are dependent claims and are not drafted in accordance with the second and third sentences of Rule 6.4(a).

Box No. III Observations where unity of invention is lacking (Continuation of item 3 of first sheet)

This International Searching Authority found multiple inventions in this international application, as follows:

Group I
Claims 1-15 are directed to an electrochemical flow cell comprising a cell body having an inlet, an outlet and a flow passage wherein a number of flow-through electrodes are disposed within the cell body transverse the flow direction.

Group II
Claim 16-30 are directed to methods of manufacturing an ultra-microelectrode comprising the steps of pulling a capillary according to a predetermined pulling profile, severing the narrowed neck of the capillary to form two separate micropipette tips and inserting an electroactive wire into the opening of at least one of the tip ends.

1. ☑ As all required additional search fees were timely paid by the applicant, this international search report covers all searchable claims.

2. ☐ As all searchable claims could be searched without effort justifying additional fees, this Authority did not invite payment of additional fees.

3. ☐ As only some of the required additional search fees were timely paid by the applicant, this international search report covers only those claims for which fees were paid, specifically claim Nos.:

4. ☐ No required additional search fees were timely paid by the applicant. Consequently, this international search report is restricted to the invention first mentioned in the claims; it is covered by claim Nos.:

Remark on Protest

☐ The additional search fees were accompanied by the applicant's protest and, where applicable, the payment of a protest fee.

☐ The additional search fees were accompanied by the applicant's protest but the applicable protest fee was not paid within the time limit specified in the invitation.

☐ No protest accompanied the payment of additional search fees.

INTERNATIONAL SEARCH REPORT
Information on patent family members

International application No.
PCT/CA2016/050314

Patent Document Cited in Search Report	Publication Date	Patent Family Member(s)	Publication Date
US5911859A	15 June 1999 (15-06-1999)	US5911859A	15 June 1999 (15-06-1999)
		AR013211A1	13 December 2000 (13-12-2000)
		CA2290968A1	28 January 1999 (28-01-1999)
		DE69821955D1	01 April 2004 (01-04-2004)
		DE69821955T2	23 December 2004 (23-12-2004)
		EP1017882A1	12 July 2000 (12-07-2000)
		EP1017882A4	29 November 2000 (29-11-2000)
		EP1017882B1	25 February 2004 (25-02-2004)
		JP2003524698A	19 August 2003 (19-08-2003)
		NO20000191D0	14 January 2000 (14-01-2000)
		NO20000191A	10 March 2000 (10-03-2000)
		WO9904063A1	28 January 1999 (28-01-1999)
CN202542927U	21 November 2012 (21-11-2012)	None	
US2012006060A1	12 January 2012 (12-01-2012)	US2012006060A1	12 January 2012 (12-01-2012)
		US8656736B2	25 February 2014 (25-02-2014)
		CN102332884A	25 January 2012 (25-01-2012)
		EP2405473A2	11 January 2012 (11-01-2012)
		EP2405473A3	03 July 2013 (03-07-2013)
		JP2012019108A	26 January 2012 (26-01-2012)
		KR20120005395A	16 January 2012 (16-01-2012)
		TW201214633A	01 April 2012 (01-04-2012)